Physical and chemical structure of planet-forming disks probed by millimeter observations and modeling

Anne Dutrey[1], Dmitry Semenov[2], Edwige Chapillon[3], Uma Gorti[4], Stéphane Guilloteau[1], Franck Hersant[1], Michiel Hogerheijde[5], Meredith Hughes[6], Gwendolyn Meeus[7], Hideko Nomura[8], Vincent Piétu[9], Chunhua Qi[10], Valentine Wakelam[1]

[1] Laboratoire d'Astrophysique de Bordeaux, CNRS, University of Bordeaux, France; [2]Max-Planck-Institut für Astronomie, Königstuhl 17, 69117 Heidelberg, Germany; [3]Institute of Astronomy and Astrophysics, Academia Sinica, P.O. Box 23-141, Taipei 106, Taiwan, Republic of China;[4]SETI Institute, 189 Bernardo Ave, Mountain View, CA 94043 USA - NASA Ames Research Center, MS 245-3, Moffett Field, CA 94035 USA;[5]Leiden Observatory, Leiden University, P.O. Box 9513, 2300 RA, Leiden, The Netherlands;[6]Wesleyan University Department of Astronomy, Van Vleck Observatory, 96 Foss Hill Drive, Middletown, CT 06459, USA;[7]UAM, Dpto. Fsica Terica, Md.15, Fac. de Ciencias, 28049, Madrid, Spain;[8]Department of Astronomy, Graduate School of Science, Kyoto University, Kyoto 606-8502, Japan ;[9]IRAM 300 rue de la Piscine, Domaine Universitaire 38406 Saint Martin d'Hres, France;[10]Harvard-Smithsonian Center for Astrophysics Cambridge, MA 02138, USA.

Protoplanetary disks composed of dust and gas are ubiquitous around young stars and are commonly recognized as nurseries of planetary systems. Their lifetime, appearance, and structure are determined by an interplay between stellar radiation, gravity, thermal pressure, magnetic field, gas viscosity, turbulence, and rotation. Molecules and dust serve as major heating and cooling agents in disks. Dust grains dominate the disk opacities, reprocess most of the stellar radiation, and shield molecules from ionizing UV/X-ray photons. Disks also dynamically evolve by building up planetary systems which drastically change their gas and dust density structures. Over the past decade significant progress has been achieved in our understanding of disk chemical composition thanks to the upgrade or advent of new millimeter/Infrared facilities (SMA, PdBI, CARMA, Herschel, e-VLA, ALMA). Some major breakthroughs in our comprehension of the disk physics and chemistry have been done since PPV. This review will present and discuss the impact of such improvements on our understanding of the disk physical structure and chemical composition.

1. INTRODUCTION

The evolution of the gas and dust in protoplanetary disks is a key element that regulates the efficiency, diversity and timescale of planet formation. The situation is complicated by the fact that the dust and gas physically and chemically interact atop of the disk structure that evolves with time. Initially, small dust grains are dynamically well coupled to the gas and are later assembled by grain growth in bigger cm-sized particles which settle towards the disk midplane (see Chapter by Testi et al.). After large grains become dynamically decoupled from the gas, they become subject to head wind from the gas orbiting at slightly lower velocities and spiral rapidly inwards or experience mutual destructive collisions. Collisionally-generated small grains are either swept out by larger grains or stirred by turbulence into the disk atmosphere. As a result, the dust-to-gas ratio and average dust sizes vary through the disk. All these processes affect the disk thermal and density structures and thus disk chemical composition.

In the dense disk midplane, thermal equilibrium between gas and dust is achieved, with dust transferring heat to gas by rapid gas-grain collisions. The disk midplane is well shielded from high-energy stellar radiation and thus is "dark", being heated indirectly via infrared emission from the upper layers, and have low ionization degree and low turbulence velocities. The ratio of ions to neutral molecules determines the level of turbulence and regulates the redistribution of the angular momentum. The outer disk midplane is so cold that many gaseous molecules are frozen out onto dust grains, leading to the formation of icy mantles that are steadily processed by cosmic rays.

Above the midplane a warmer, less dense region is located, where gas-grain collisional coupling can no longer be efficient, and dust and gas temperatures start to depart from each other, with the gas temperature being usually higher. The intermediate disk layer is only partly shielded from the ionizing radiation by the dust and thus is more ionized and dynamically active than the midplane. Rich gas-phase and gas-grain chemistries enable synthesis of many molecules in this so-called molecular layer.

Finally, in the heavily irradiated, hot and dilute atmosphere only simple atoms, ions, photostable radicals and PAHs are able to survive. The global chemical evolution is dominated by a limited set of gas-phase reactions in this disk region.

Observations of protoplanetary disks of various ages and sizes surrounding Sun-like and intermediate-mass stars help to resolve some of the related ambiguities. Detailed studies of protoplanetary disks remain an observationally chal-

lenging task though, as disks are compact objects and have relatively low masses. At visual and infrared wavelengths disks are typically opaque, and one uses (sub-)millimeter imaging with single-dish telescopes and antenna arrays to peer through their structure. Since observations of the most dominant species in disks, H_2, are impossible (except of the hot upper layers via its weak quadrupole IR transitions or of the inner disk via the fluorescent FUV lines), other molecules are employed to trace disk kinematics, temperature, density, and chemical structure. The poorly known properties such as (sub-)millimeter dust emissivities and dust-to-gas ratio make it hard to derive a total disk mass from dust emission alone. Apart from a handful of simple molecules, like CO, HCO^+, H_2CO, CS, CN, HCN and HNC, the molecular content of protoplanetary disks remains largely unknown.

In the last ten years, upgraded and new millimeter (mm) or submillimeter (submm) facilities (IRAM, CARMA, SMA, Herschel and ALMA) have permitted the detection of a few other molecular species (DCN, N_2H^+, H_2O, HC_3N, C_3H_2, HD) at better spatial and frequency resolution. In the meantime, disk models have benefited from improvements in astrochemistry databases (like KIDA and UDFA'12), development of coupled thermo-chemical disk physical models, line radiative transfer codes, and better analysis tools. The spatial distribution of molecular abundances in disks is still poorly determined, hampering a detailed comparison with existing chemical models. Due to the complexity of the molecular line excitation, unambiguous interpretation of the observational results necessitates advanced modeling of the disk physical structure and evolution, chemical history, and radiative transfer.

Figure 1 illustrates the state of art prior to the Protostars and Planets VI conference hold in Heidelberg in June 2013. The disk structure (density and temperature) has been calculated for a T Tauri star with the mass of $1\,M_\odot$. With the exception of the very inner disk ($R \leq 10$ AU), where dissipation of accretion energy can be a source of mechanical heat, disks are mostly heated by the stellar radiation, including UV and X rays, the interstellar UV field and the cosmic rays. Both the gas and dust have vertical and radial temperature gradients, the upper disk layers being super-heated by the central star(s). As grains grow and rapidly settle towards the disk midplane (see Chapter by Testi et al.), the vertical temperature gradient changes and the midplane further cools off. This may have impact on the location and size of the freeze-out zones of various molecules, where they mainly remain bound to the dust grains.

In summary, there are three different chemical zones in disks: (1) the disk upper layer that is similar to a dense PDR, which consist of simple ions, neutral species, and small dust grains, (2) the warm intermediate molecular layer with many molecules (including some complex ones) in the gas phase and rapid gas-dust interactions, and (3) the cold midplane devoid of many gaseous molecules but icy-rich at radii $\gtrsim 20 - 200$ AU, similar to dense prestellar cores.

This review will present the recent improvements on our understanding of disk physical structure and chemical composition, and their evolution with time, both from the observational but also theoretical perspectives. Other recent comprehensive reviews on the subject of disk physics and chemistry are those by *Bergin* (2011), *Semenov* (2010) and *Henning and Semenov* (2013).

2. DATA ANALYSIS AND BIAS

The physical structure of protoplanetary disks is so unique because it has both the strong density and temperature gradients on relatively short spatial scales. For example, at a radius of 100 AU, the midplane temperature is expected to be around 7-12 K, while at the 1-3 scale heights (H) above (at about 15-50 AU), the temperature is warm enough to facilitate the presence of a molecular layer. In the meantime, the gas density drops by about one to four orders of magnitude. As a consequence, the chemical conditions change rapidly along the line of sight, as well as the excitation conditions, leading in some cases to non-LTE effects. Last but not least, a proper analysis of any line detection in disks requires an adequate handling of the line formation process, including possible non-LTE excitation, but also gas kinematics, in particular, the disk Keplerian shear (*Guilloteau et al.* 2006; *Dutrey et al.* 2007a).

Line analysis falls in two main categories: inversion methods, which attempt to retrieve the physical parameters (e.g. the excitation temperature, the molecular surface density distributions, etc..) and their confidence intervals, and forward modeling, which evaluate whether a given model can represent the observations. In the radiative transfer codes used to analyze observations or predict mm/submm line emissions, the physical parameters (density, gas temperature, scale height or turbulence) are usually specified as explained below:

Temperature: Disk temperature is treated in three main ways: 1) the gas temperature is assumed to be isothermal in the vertical direction and to follow a power law in the radial direction, $T_k(r) \propto r^{-q}$ (*Dutrey et al.* 1994), 2) a vertical gradient is also included (*Dartois et al.* 2003; *Qi et al.* 2011; *Rosenfeld et al.* 2012), using simple parametrization of dust disk models possibly with the use of a simplified approach to the radiative transfer problem (*Chiang and Goldreich* 1997; *D'Alessio et al.* 1998), or 3) the temperature is directly calculated by the dust radiative equilibrium modeling (*Pinte et al.* 2008; *Isella et al.* 2009). This last category of models has a number of hidden and often not well constrained parameters. The surface density distribution must be specified, as well as the dust properties (minimum and maximum radii, size distribution index, composition) to calculate the dust absorption coefficients. These models can accommodate grain growth and even dust settling (e.g. *Dullemond et al.* 2007; *Hasegawa and Pudritz* 2010b; *Williams and Cieza* 2011). The dust disk properties are usually adjusted to fit the the Spectral Energy Distribution

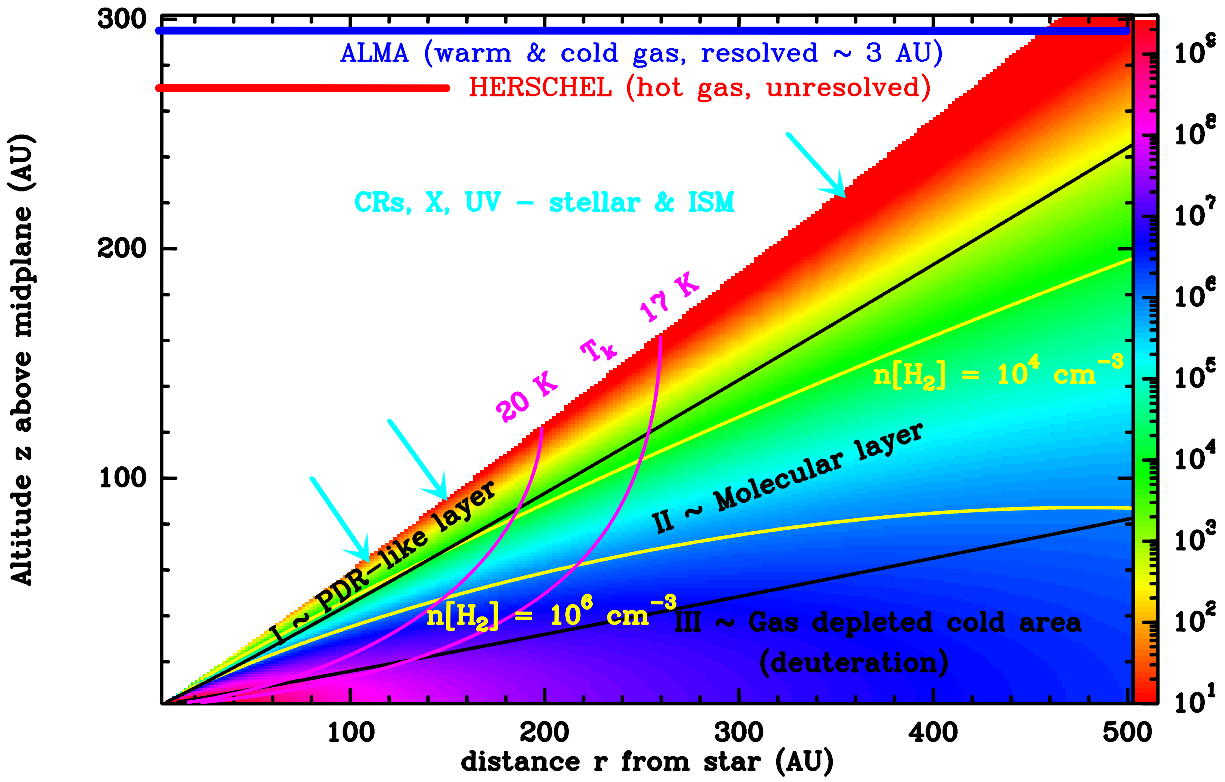

Fig. 1.— Molecular disk: state of art after PPV. The model is done for a disk orbiting a young star of one solar mass. The volume density as a function of radius r and altitude z above the midplane is given in color. The location of the isotherms at 17 and 20 K are also shown. I,II and III correspond to the location of the three important layers of gas: the PDR-like atmosphere irradiated by the star, the UV interstellar field and the cosmic rays (I), the molecular layer typically located between one and three scale heights (II), and the midplane where only molecular hydrogen and deuterated isotopologues of simple molecules are abundant in the gas phase (III). Top lines: the red line gives the area sampled by Herschel observations (unresolved). The blue line corresponds to the area sampled by ALMA (with the best resolution for a source at 150 pc).

(SED), sometimes simultaneously with resolved dust maps in the mm/submm (*Isella et al.* 2009; *Gräfe et al.* 2013). A last refinement is to also evaluate the gas heating and cooling and to account for the differences between the gas and dust temperature as a function of disk location (this will be discussed in Section 4.1).

Density: Two types of surface density must be considered: the total (mass) surface density and individual molecule distributions. Some parametric models allow to adjust the molecular distributions, either as power law surface densities (*Piétu et al.* 2007), or more sophisticated variations, such as piece-wise power law integrated abundance profiles (*Qi et al.* 2008; *Guilloteau et al.* 2012) atop of a prescribed H_2 surface density. In forward modeling, models computing the thermal balance (dust and/or gas) in general assume a power law (mass) surface density profile. Exponentially tapered profiles have also been invoked to explain the different radii observed in CO isotopologues (*Hughes et al.* 2009), but are not widely used in forward modeling.

Scale height: The gas is usually assumed to be in hydrostatic equilibrium. The scale height is prescribed as a power law or self-consistently calculated from the temperature profile, but the feedback of the temperature profile on the vertical density profile is neglected in most cases. The scale height can be expressed as (e.g. *Dartois et al.* 2003; *Dutrey et al.* 2007b):

$$H(r) = \sqrt{\frac{2kr^3T(r)}{GM_*m_0}} = \sqrt{\frac{2k}{m_0}}\frac{r}{V_{\rm K}(r)}\sqrt{T(r)} = \sqrt{2}c_{\rm s}/\Omega, \quad (1)$$

where $T(r)$ is the kinetic temperature, M_* is the stellar mass, m_0 is the mean molecular weight of the gas, $V_{\rm K}(r)$ is the Keplerian velocity, $c_{\rm s}$ is the sound speed, and Ω is the angular velocity.

Self-consistent calculation of the hydrostatic equilibrium with vertical temperature gradients is however taken into account in some models (e.g. *D'Alessio et al.* 1998; *Gorti and Hollenbach* 2004).

Turbulence: Turbulence is usually mimicked as by setting the local line width $\Delta V = \sqrt{v_{th}^2 + v_{turb}^2}$ where v_{th} is the thermal broadening and v_{turb} the turbulent term (*Dartois et al.* 2003; *Piétu et al.* 2007; *Hughes et al.* 2011).

Excitation conditions: The first rotational levels of most of the simple molecules observed so far with current arrays such as CO, HCO^+, CN and HCN should be thermalized in the molecular layer, given the expected H_2 densities. This strongly simplifies the analysis of the data. This is however less true for higher levels (above J=3), as noted by *Pavlyuchenkov et al.* (2007), and a correct treatment of the non-LTE excitation conditions is needed. These non-LTE effects will become more common with submm ALMA (Atacama Large Millimetre Array) observations sensitive to weaker lines and to more warmer, inner disk regions with strong dust continuum background emission.

Thermo-chemical models: The most sophisticated approach is to couple the calculation of the thermal and density structures to the derivation of the chemistry to make molecular line predictions (*Woitke et al.* 2009b; *Kamp et al.* 2010; *Akimkin et al.* 2013). However, the computing requirements limit this kind of approach to forward modeling only. Despite the interest of such models to understand the role of various processes, it is important to remember that they also have their own limitations, such as the use of equilibrium chemistry, the choice of dust properties, or an underlying surface density profile. We review these models in Section 4.1.

2.1 Unresolved Data

For most unresolved data, the SED at near-, mid-, and far-infrared and (sub-)millimeter wavelengths is commonly used to derive the disk structure from radii < 1 AU all the way to the outer radius (*Dullemond et al.* 2007), as the SED traces the distribution of the dust in the disk. The dust is supported by the gas, so information on the gas radial distribution and scale heights can also be derived. However, this assumes that the dust is dynamically coupled to the gas, which is only true for small particles ($\lesssim 100\mu$m). Complicating details are the presence of multiple dust populations, vertical settling and radial drift of dust constituents, generally poorly constrained dust opacities (see also Testi et al. chapter), and the gas and dust thermal decoupling.

Moreover, the IR part of the SED is in general insensitive to the total dust content, which is only constrained by the (sub-)mm range. Neither of them is sensitive to the disk outer radius. Spatially integrated, spectrally resolved line profiles can be the tools to sample disk properties, because the line formation in a Keplerian disk links velocities to radial distances. This can be used to obtain disk radii (*Guilloteau et al.* 2013) or evidence for central holes (*Dutrey et al.* 2008, , see also Sec.5).

2.2 Resolved Interferometric Data

Resolved interferometric molecular maps on nearby protoplanetary disks are routinely obtained from most mm/submm arrays such as the SMA (Submillimetre Array), CARMA (Combined Array for Research in Millimeter-wave Astronomy) and IRAM (Intitut de RadioAstronomie Millimetrique) Plateau de Bure Interferometer (PdBI).

The UV coverage of these facilities is still a limiting factor and data are generally compared to disk models by χ^2 minimizations performed in the Fourier plane in order to avoid non linear effects due to the deconvolution. This later step should no longer be necessary for most ALMA configurations.

Other important limitations are due to the assumed density and temperature laws. Current arrays do not have enough sensitivity and angular resolution to allow a fine determination of the radial and vertical structure. Depending on the way the temperature is calculated (from the dust) or determined (from thermalized CO lines such the 1-0 or the 2-1 transitions), the biases are different. In the first case, the gas temperature is directly dependent on the poorly known dust properties, and there is no direct gas temperature measurements. In the second case, an excitation temperature is determined, but its interpretation as the kinetic temperature depends on the robustness of the LTE hypothesis, and the region sampled by the measurement, as it is depends on the chemical behavior of the observed molecule.

3. MOLECULAR OBSERVATIONS

We discuss in this section how molecular observations obtained at mm/submm wavelengths can constrain the disk structures. Some far-IR results obtained mostly with Herschel are also discussed but the gas properties of the warm surface and inner disk derived from IR observations (Spitzer, Herschel) are discussed in the chapter by Pontoppidan et al.

3.1 Detected Species

Since H_2 cannot be used as a tracer of the bulk of gas mass, the study of the more abundant molecules after H_2 is mandatory to improve our knowledge on the gas disk density and mass distribution. After the detection of a few simple molecules in the T Tauri disks surrounding the 0.5 $M_\odot$ DM Tau and the binary system GG Tau (1.2 $M_\odot$) by *Dutrey et al.* (1997), millimeter/submmilliter facilities have observed several protoplanetary disks around young stars with mass ranging between $\sim$ 0.3 and 2.5 $M_\odot$ (e.g. *Kastner et al.* 1997; *Thi et al.* 2004). The main result of mm/submm molecular studies is that detections are limited to the most abundant molecules found in cold molecular clouds: CO (with ^{13}CO and C^{18}O), HCO$^+$ (with H^{13}CO$^+$ and DCO$^+$), CS, HCN (with HNC and DCN), CN, H_2CO, N_2H^+, C_2H and, very recently, HC_3N (*Chapillon et al.* 2012b) followed by the detection of cyclic C_3H_2 in the disk surrounding HD 163296 using ALMA (see Fig.3; *Qi et al.* 2013a). H_2O has also been detected by the Herschel satellite in TW Hya and DM Tau (marginal detection) (*Bergin et al.* 2010; *Hogerheijde et al.* 2011), while the main reservoir of elemental deuterium, HD, has been detected in TW Hya by *Bergin et al.* (2013). The mm/submm molecular detections are summarized in Table 1.

3.2 Outer Disks Structure ($R > 30$ AU)

CO as a tracer of the disk structure: Resolved spectro-imaging observations of CO isotopologues have been so far the most powerful method to constrain the geometry (outer radius, orientation and inclination) and velocity pattern of protoplanetary disks (*Koerner et al.* 1993; *Dutrey et al.* 1994; *Guilloteau and Dutrey* 1998).

As the first lowest rotational levels of CO are thermalized, the observations of the J=1-0 and J=2-1 transitions permit a direct measurement of the gas temperature and surface densities. Furthermore, because of their different opacities, the ^{12}CO, ^{13}CO J=1-0 and J=2-1 lines sample different disk layers, probing the temperature gradient as a function of height (see *Dutrey et al.* 2007b, for a detailed discussion). With the optically thicker lines (e.g. ^{12}CO J=2-1), the temperature can be measured in a significant disk fraction, while the estimate of the molecular surface density is only possible in the outer optically thin region (*Dartois et al.* 2003; *Piétu et al.* 2007).

Temperature structure: Closer to the midplane, several studies on various molecular lines such as CCH 1-0 and 2-1 (*Henning et al.* 2010), HCN 1-0 and CN 2-1 (*Chapillon et al.* 2012a) and CS 3-2 (*Guilloteau et al.* 2012) suggest that the gas is cold, with apparent temperatures of the order of $\sim 10 - 15$ K at 100 AU for T Tauri disks. As this is below the CO freeze-out temperature (17 - 19 K), CO and most other molecules should be severely depleted from the gas phase (apart from H_2, H_3^+ and their deuterated isotopologues). Disks around HAe stars appear warmer (*Piétu et al.* 2007). To explain the low molecular temperatures observed in the T Tauri disks, several possibilities can be invoked. With the physical structure predicted by standard disk models, the observed molecular transitions of CN, CCH, HCN and CS should be thermalized in a large area of these disks. Hence, a subthermal excitation for these is unlikely, especially as the derived low temperatures are similar to those obtained from (thermalized) CO 1-0 and 2-1 transitions (*Piétu et al.* 2007). *Chapillon et al.* (2012a) have also investigated the possibility to have a lower gas-to-dust ratio (by about a factor $\sim$ 6). In that case subthermal excitation becomes possible but the predicted column densities for HCN and CN are low compared to the observed ones. Turbulence may play a role by transporting gaseous molecules into the cold midplane regions on a shorther timescale than the freeze-out timescale (*Semenov et al.* 2006; *Aikawa* 2007), but may be insufficient (*Hersant et al.* 2009; *Semenov and Wiebe* 2011), see also Sect.4.2.2.1. Finally, another possibility would be that "cold" chemistry for molecules such as CN or CCH, and in particular photo-desorption rates, are poorly known (*Öberg et al.* 2009a; *Hersant et al.* 2009; *Walsh et al.* 2012). Tracing the very cold midplane is challenging since most molecules should be frozen onto grains. The best candidate to trace this zone are the H_2D^+ or D_2H^+ ions, because of their smaller molecular masses, but they remain to be detected in protoplanetary disks (see Sect. 5.3 and Ceccarelli et al. chapter in this book).

Higher in the disk, higher transitions of CO permit to constrain the vertical structure. Using CO 3-2 and 6-5 maps

TABLE 1
A TABLE OF DETECTED SPECIES IN T TAURI (COLD) AND HERBIG AE (WARM) OUTER DISKS USING MM/SUBMM FACILITIES

Species	T Tauri cold disk $T < 15$ K at $R > 50$ AU	Herbig Ae warm disk $T < 15$ K at $R > 200$ AU	Telescope
CO, ^{13}CO, C^{18}O	Many	Many	Many
CN	Many	Many	Many
HCN, HNC	Several, DM Tau		IRAM, SMA
DCN	TW Hydra	-	SMA, ALMA
CS	Several	Several	IRAM, SMA
C_2H	Several	Several	IRAM, SMA
H_2CO	Several	A few	IRAM, SMA
HCO^+	Several	Several	IRAM, SMA
DCO^+	TW Hya, DM Tau	HD 163296	IRAM, SMA
N_2H^+	3-4	HD 163296	IRAM, SMA, ALMA
HC_3N	3-4		IRAM
c-C_3H_2	-	HD 163296	ALMA
H_2O	TW Hya, DM Tau		Herschel
HD	TW Hya		Herschel

obtained with the SMA, *Qi et al.* (2004, 2006) have investigated the temperature and the heating processes in the T Tauri disk surrounding TW Hya. They found that the intensity of CO 6-5 emission can only be explained in presence of additional heating by stellar UV and X-rays photons.

While a significant fraction of T Tauri disks exhibits low gas temperatures, several studies of Herbig Ae disks found that these disks are warmer, as predicted by the thermo-chemical disk models. *Piétu et al.* (2007) and *Chapillon et al.* (2012a) found from the CO, HCN and CN studies with the PdBI that the molecular disk surrounding MWC 480 has a typical temperature of about 30 K at radius of 100 AU around the midplane. In the case of HD 163296, *Qi et al.* (2011) used a multi-transition and multi-isotopologues study of CO (from SMA and CARMA arrays) to determine the location CO snowline, where the CO column density changes by a factor 100. They found a radius of $\sim$ 155 AU of this snowline. This result, consistent with the SMA observation of H_2CO (*Qi et al.* 2013b), is confirmed by the ALMA observation of DCO^+ (*Mathews et al.* 2013). More recently, *Qi et al.* (2013c) found that the CO snowline in TW Hya is likely located at a radius $\sim$ 30 AU, where the inner edge of N_2H^+ ring is detected. This N_2H^+ ring is the result of an increase in N_2H^+ column density in the region where CO abundances are low, because CO efficiently destroys N_2H^+ by the proton transfer reaction: $N_2H^+ + CO \rightarrow N_2 + HCO^+$.

Molecular density structure: The chemical behavior and the associated abundance variations of the molecules used to characterize the gas precludes an absolute determination of the gas mass. Recently, the far-infrared fundamental rotational line of HD has been detected in the TW Hya disk with *Herschel* (*Bergin et al.* 2013). The abundance distribution of HD closely follows that of H_2. Therefore, HD, which has a weak permanent dipole moment, can be used as a direct probe of the disk gas mass. The inferred mass of the TW Hya disk is $\gtrsim 0.05 M_\odot$, which is surprising for a $3-10$ Myr old system. Other detections of HD using SOFIA could be a very powerful way to directly constrain the gas mass, assuming the thermal structure is reasonably known.

Whereas the absolute determination of the gas mass is not yet possible, the radial and vertical distributions of the molecular gas are better known. Several complementary studies of the gas and dust distributions assuming either power law or exponential decay for the surface density distribution have been recently performed (*Isella et al.* 2009; *Hughes et al.* 2009, 2011; *Guilloteau et al.* 2011). Most of these studies are based on the analysis of dust maps (see also chapter by Testi et al.) but these results are still limited in sensitivity and angular resolution.

The vertical location of the molecular layer was investigated in several studies, but in an indirect way. *Piétu et al.* (2007) found that the apparent scale heights of CO are larger than the expected hydrostatic value in DM Tau, LkCa 15 and MWC 480. *Guilloteau et al.* (2012) showed that the CS 3-2 and 5-4 PdBI maps are best explained if the CS layer is located about one scale height above the midplane, in agreement with model predictions. However, the first *direct* measurement of the location of the molecular layer has only been recently obtained with ALMA observations of HD 163296, where the CO emission clearly originates from a layer at $\sim 15^\circ$ above the disk plane (*Rosenfeld et al.* 2013; *de Gregorio-Monsalvo et al.* 2013), at a few

hundred AU.

Gas-grain coupling: Several observational studies indicate the importance of the grain surface chemistry for disks.

Using the IRAM 30-m telescope, *Dutrey et al.* (2011) failed to detect SO and H_2S in DM Tau, GO Tau, LkCa15 and MWC480 disks. They compared the molecular column densities derived from the observations with chemical predictions made using Nautilus (*Hersant et al.* 2009) and the density and temperature profiles taken from previous analysis (e.g. *Piétu et al.* 2007). They reproduced the SO upper limits and CS column densities reasonably well, but failed to match the upper limits obtained on H_2S by at least one order of magnitude. This suggests that at the high densities and low temperatures encountered around disk midplanes, H_2S remains locked onto the grain surfaces and where it also gets destroyed to form other species. Indeed, some recent experiments by *Garozzo et al.* (2010) have shown that H_2S on grains is easily destroyed by cosmic rays and lead to the formation of C_2S, SO_2 and OCS on grains. These studies also suggest that most of the sulphur may be in the form of a sulphur rich residuum, which could be polymers of sulfur or amorphous aggregates of sulfur (*Wakelam et al.* 2004). The associated grain surface reactions are not yet incorporated in chemical models.

The low apparent CO to dust ratio observed in all disks has in general been attributed to the freeze-out of CO onto the dust grains in the outer disk regions at $r \gtrsim 200$ AU with $T \lesssim 20$ K. The importance of this mechanism is demonstrated by the observations of CO isotopologues in the HD 163296 disk by *Mathews et al.* (2013). However, this mechanism, although unavoidable, may not be sufficient to explain the low CO content. Strong apparent CO depletion (factor ~ 100) has also been observed in warm disks, with temperatures above 30 K, where thermal desorption should occur: the disks around the Herbig stars CQ Tau and MWC 758, *Chapillon et al.* (2008), and BP Tau (*Dutrey et al.* 2003). *Chapillon et al.* (2008) suggested that CO may have been removed from the gas phase during the cold pre-stellar phase by adsorption on small grains. During the warmer protostellar phase, grain growth occurs, and CO may stay locked in the ice mantles of large grains that may remain sufficiently colder than small grains during the reheating phase. Also, from a complete modelling of CO isotopologues in TW Hya, *Favre et al.* (2013) concluded that depletion alone could not account for the low CO to H_2 ratio, the H_2 content being derived from detection of HD (*Bergin et al.* 2013). They invoke CO conversion to carbon chains, or perhaps CO_2, that can remain locked in ice mantles at higher temperature than CO.

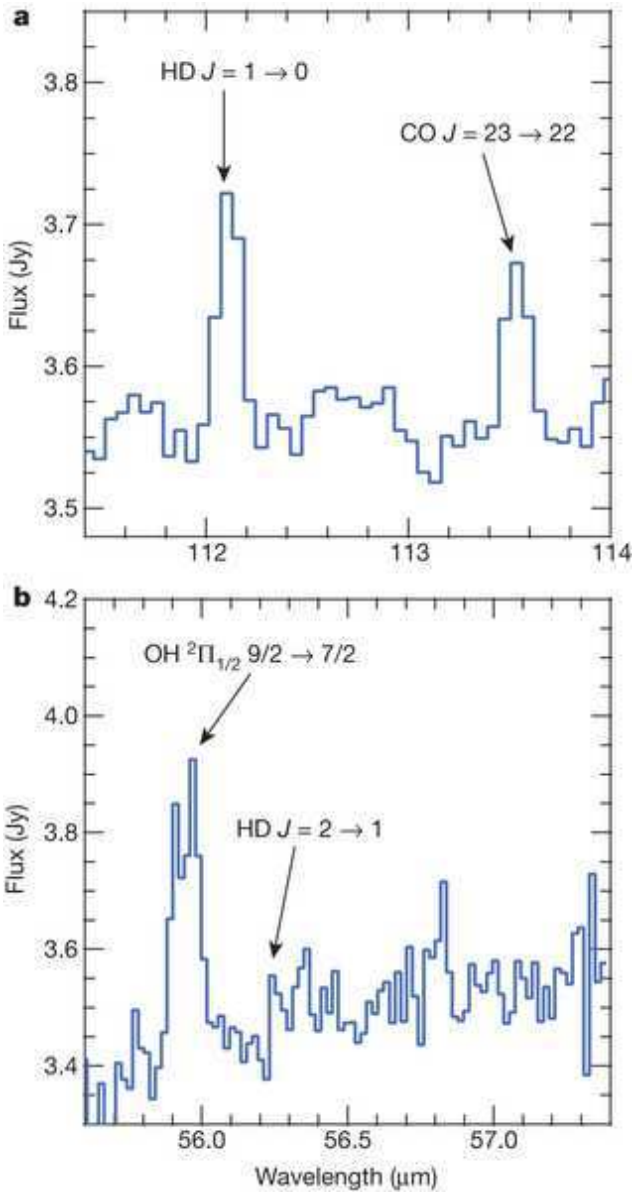

Fig. 2.— From *Bergin et al.* (2013). Hydrogen Deuteride around TW Hydra observed with Herschel. The HD J=1–0 line at 112μm (a) is detected at 5σ level, while there is only an upper limit on the HD J=2–1 line (b).

Molecular complexity: Prior to ALMA, with the exception of HC_3N (*Chapillon et al.* 2012b), the molecules which have been detected are the simplest, lighter molecules. *Qi et al.* (2013a) recently report the detection with ALMA of c-C_3H_2 in the warm disk surrounding the Herbig Ae star

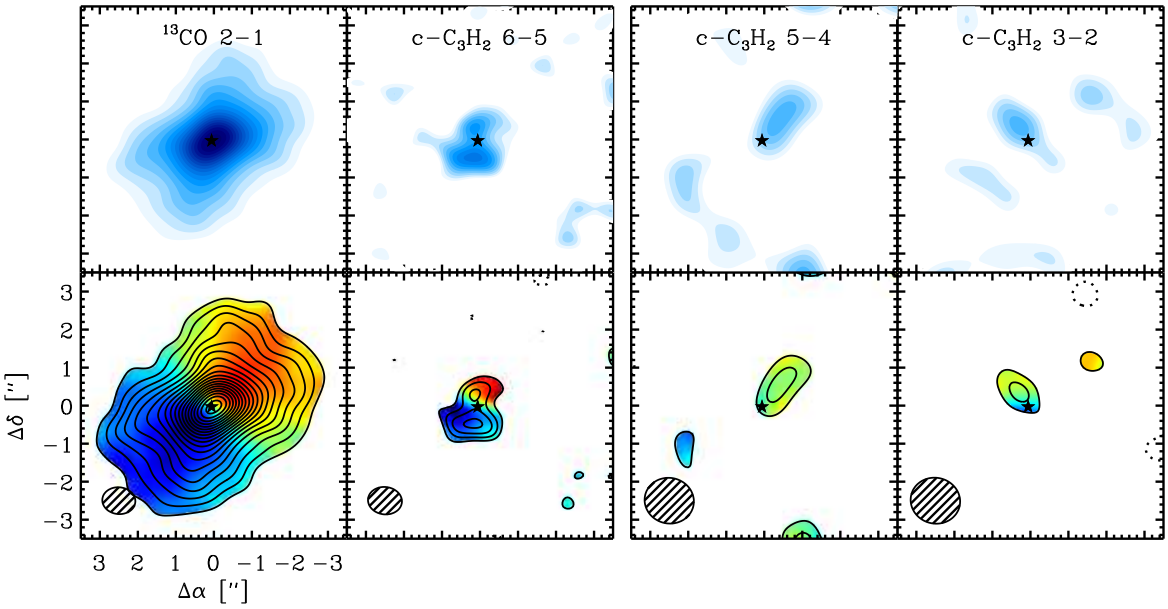

Fig. 3.— From *Qi et al.* (2013a). The integrated intensity maps and and intensity-weighted mean velocity fields of ^{13}CO 2-1 and c−C_3H_2 6-5 lines (left panels), as well as c-C_3H_2 5-4 and 3-2 lines (right panels) toward HD 163296. The resolved velocity field of the c−C_3H_2 6-5 line agrees with the CO kinematics. In the c−C_3H_2 maps, the first contour marks 3σ followed by the 1σ contour increases. The rms varies between 6 and 9 mJy.km/s per beam. Synthesized beams are presented in the lower left corners. The star symbol denotes the continuum (stellar) position. The axes are offsets from the pointing center in arc-seconds.

HD 163296 (see Fig.3).

Perspectives: A major challenge of ALMA will be to refine our knowledge on the vertical and radial structure by studying the excitation conditions through multi-isotope, multi-transition studies of several molecular tracers such as CN, CS, HCO^+ or HCN at a high angular resolution. Particularly, the CO isotopologues will remain robust tracers of the disk structure. Defining the physical conditions in the midplane will likely remain difficult and should require long integration time to detect species such as H_2D^+, DCO^+ or N_2D^+.

3.3 Inner Disk Structure (<30 AU)

Unlike the outer disk, the inner (<30 AU) disk has remained unresolved with (sub-)millimeter interferometers (see e.g. *Dullemond and Monnier* 2010). In the near future, the longest baselines of ALMA will start to image these regions, but up to now all information about molecular gas has been obtained from *spatially* unresolved observations. However, *spectrally* resolved observations can be used to establish the region from which line emission originates if a Keplerian velocity curve is assumed. Infrared interferometry provides information on the innermost regions at radii of $<$ 1 AU (e.g. *Kraus et al.* 2009), but has been mostly limited to continuum observations, with the exception of several solid-state features (e.g. *van Boekel et al.* 2004).

SED modeling also provides at first order a good description of the density and temperature structure of the dust throughout the disk. However, especially in the inner disk and also at several scale heights, gas temperatures may exceed dust temperatures because of high-energy radiation (*Kamp and Dullemond* 2004). The (local) gas-to-dust ratio, dust-size distribution and the effects of dust settling are all factors in determining the relative dust and gas temperatures, and complicate the interpretation of molecular line observations of the inner disk. Of particular interest for the inner disk are constraints on any gaps present in this region (e.g. *Maaskant et al.* 2013) and the shape of the gap walls (*McClure et al.* 2013) that depend on the gap-opening mechanism and accretion (*Mulders et al.* 2013). The disk gaps and inner holes provide a directly irradiated, warm surface visible in excited molecular lines, and the question whether any gas remains in these regions (see Chapters by Espaillat et al. and Pontoppidan et al.).

In recent years, the HIFI and PACS instruments on the Herschel Space Observatory have probed the inner disks through spatially unresolved, but, in the case of HIFI, spectrally resolved, emission lines of gas species and several solid-state features from the dust. Several authors (*Meeus et al.* 2012; *Riviere-Marichalar et al.* 2012, 2013; *Fedele et al.* 2012) present Herschel observations of H_2O, CO, [O I], OH, CH^+ and [C II] lines from T Tauri and Herbig Ae/Be disks. Atomic oxygen is firmly detected in most disks and correlates with the far-IR dust continuum, CO is observed in $\sim$ 50% of disks and is stronger in flaring

disks, while [C II] emission is often not confined to the disk and difficult to separate from the surrounding environment (*Fedele et al.* 2012, 2013). H_2O and OH lines are only observed in a few Herbig stars (*Meeus et al.* 2012; *Fedele et al.* 2012), while they are strong in T Tauri stars with outflows (*Podio et al.* 2012). Furthermore, the emission of hot water located around 2–3 AU is observed in 24% of gas-rich T Tauri disks (*Riviere-Marichalar et al.* 2012). Lastly, CH^+, tracing hot gas was discovered in two Herbig stars with high UV flux: HD 97048 and HD 100546 (*Thi et al.* 2011a; *Meeus et al.* 2012).

Using thermo-chemical models with a disk structure derived from continuum observations, it was shown that these lines probe the inner disk as well as the upper disk layers directly illuminated, and heated, by ultraviolet radiation, where PAH heating can play an important role (e.g. *Woitke et al.* 2010; *Bruderer et al.* 2012). Herbig stars and the T Tauri stars have an important difference in this context: while in Herbig stars the UV radiation is stellar, in T Tauri stars it is mainly due to accretion shocks. Almost universally, these lines show that the gas in the upper disk regions is warmer than the dust (e.g. *Kamp and Dullemond* 2004; *Bruderer et al.* 2012), in accordance with models including photon heating (PDRs). Considering multiple transitions of CO in the HD 100546 disk, *Fedele et al.* (2013) found a steeper temperature gradient for the gas compared to the dust, providing further direct proof of thermal decoupling between gas and dust. *Aresu et al.* (2012) showed that the [O I] line flux increases with UV flux when $L_X < 10^{30}$ erg s^{-1}, and with increasing L_X (when it is higher that the UV luminosity). *Thi et al.* (2011a) detected CH^+ in HD 100546, and concluded that this species is most abundant at the disk rim at 10–13 AU. In HD 163296, *Tilling et al.* (2012) studied the effect of dust settling, and found that in settled models the line fluxes of species formed deeper in the disk are increased. *Thi et al.* (2013) found that the line observations of the disk around 51 Oph can only be explained if is compact (<10–15 AU), although an outer, cold disk devoid of gas may be extended up to 400 AU. For all these lines observed with Herschel, it is good to remember that, while they dominate the far-infrared spectrum, they only trace a small fraction of the disk, and that the dominant disk mass reservoir near the midplane at these radii is much cooler and will require high-resolution millimeter (ALMA) observations.

Solid-state features present in the Herschel wavelength range provided information about the dust composition of the inner disk. Emission of the 69 μm forsterite feature in the disk of HD 100546 (*Sturm et al.* 2010, 2013) was shown by *Mulders et al.* (2011) to be dominated by emission from the inner disk wall located between 13–20 AU. Detailed modeling of the line shape of the feature yielded a crystalline mass fraction of 40–60% in this region, with a low iron content of <0.3%.A tentative detection of crystalline water ice using PACS was also reported by *McClure et al.* (2012) in the disk surrounding the T Tauri star GQ Lup.

The chapter of Pontoppidan et al. in this volume extensively discusses the volatile content of disks. Here we only mention that significant decrease of the H_2O abundances across the expected snowline has been observed in several disks using unresolved Herschel and Spitzer observations (e.g. *Meijerink et al.* 2009; *Zhang et al.* 2013). *Najita et al.* (2013) and *Qi et al.* (2013b) concluded that species such HCN, N_2H^+, and H_2CO reveal the presence of H_2O and CO snowlines through chemical signatures.

Intriguing conclusions can be drawn from spatially unresolved observations using spectrally resolved emission lines, when an underlying Keplerian velocity profile is assumed. Using Science Verification data from ALMA and the high signal-to-noise CO line data, *Rosenfeld et al.* (2012) found that the inner disk of TW Hya is likely warped by a few degrees on scales of 5 AU. Such a warp is consistent with what was earlier deduced by optical scattered light (*Roberge et al.* 2005), and may be explained by a (planetary?) companion inside the disk.

With the roll-out of ALMA, high sensitivity imaging of regions as small as a few AU will become feasible, providing direct information on the region where planets form.

4. THERMO-CHEMICAL PROCESSES

Protoplanetary disks are characterized by strong vertical and radial temperature and density gradients and varying UV/X-ray radiation intensities. These conditions favors diverse chemical processes, including photochemistry, molecular-ion reactions, neutral-neutral reactions, gas-grain surface interactions, and grain surface reactions. Local density, temperature and high-energy irradiation determine which of these processes will be dominating.

Disk chemistry is driven by high-energy radiation and cosmic rays (*Aikawa and Herbst* 1999; *Aikawa et al.* 2002; *van Zadelhoff et al.* 2003; *Gorti and Hollenbach* 2004; *van Dishoeck* 2006; *van Dishoeck et al.* 2006; *Fogel et al.* 2011; *Vasyunin et al.* 2011; *Walsh et al.* 2012; *Akimkin et al.* 2013). T Tauri stars possess intense non-thermal UV radiation from the accretion shocks, while the hotter Herbig Ae/Be stars produce intense thermal UV emission. The overall intensity of the stellar UV radiation at 100 AU can be higher by a factor of $100 - 1\,000$ for a T Tauri disk (*Bergin et al.* 2003) and 10^5 for a Herbig Ae disk (*Semenov et al.* 2005; *Jonkheid et al.* 2006), respectively, compared to the interstellar radiation field (*Draine* 1978). Photodissociation of molecules will depend sensitively on the shape and strength of the UV radiation field. For example, Lyman α photons will selectively dissociate HCN and H_2O, while other molecules that dissociate between 91.2 and 110 nm such as CO and H_2 remain unaffected (*van Dishoeck and Black* 1988; *van Dishoeck et al.* 2006). Selective photodissociation of CO by the interstellar radiation field can also play an important role in the outer disk region (*Dartois et al.* 2003).

The $\sim 1 - 10$ keV X-ray radiation is another important energy source for disk chemistry. The median value for the

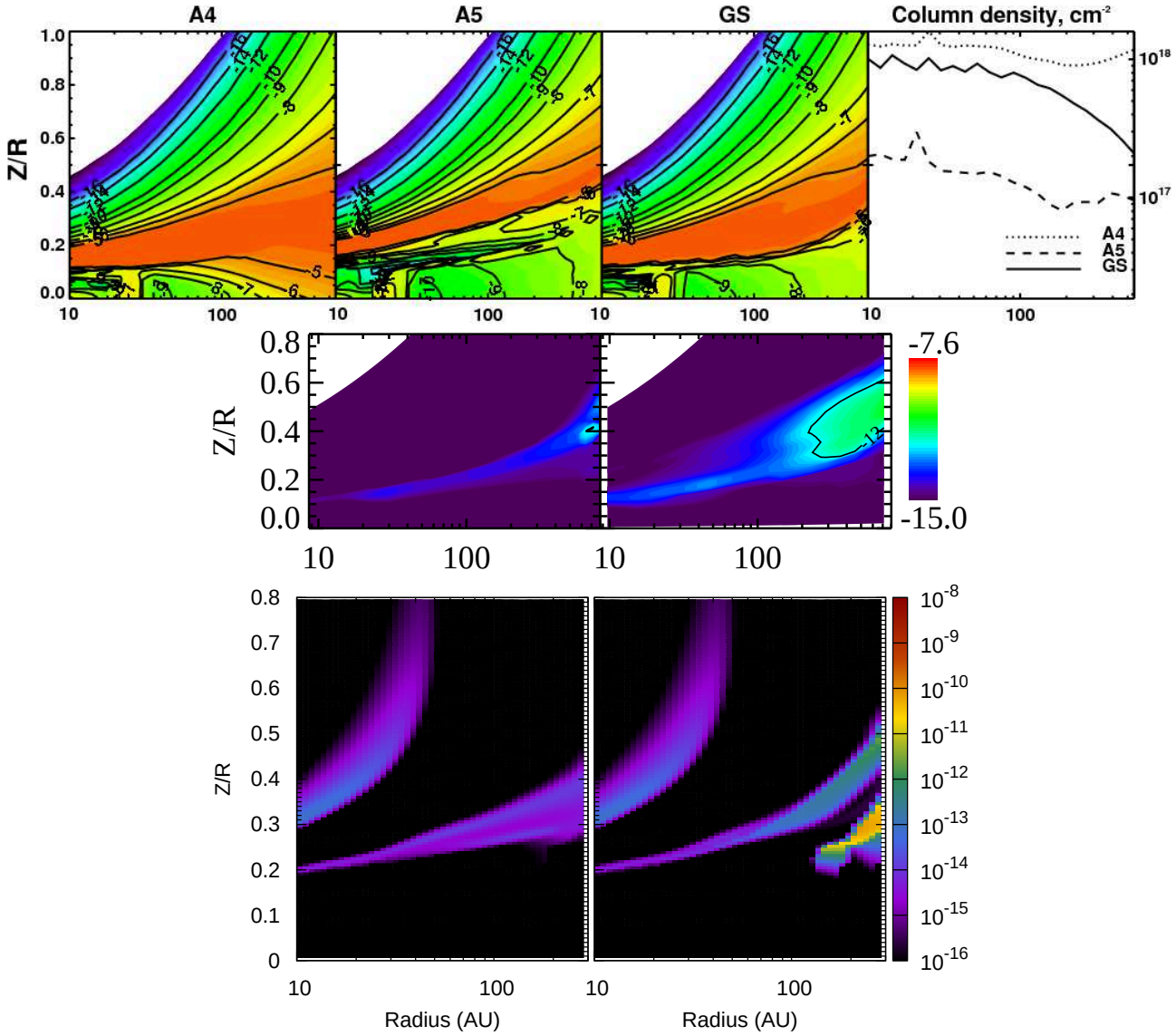

Fig. 4.— Top panel: Fractional abundance profiles (first three columns) and column densities (fourth column) of the gas-phase carbon monoxide in a T Tauri disk calculated with three distinct dust grain models: (A4) the uniform grains with radius of 1 μm, (A5) the uniform grains with radius of 0.1 μm and (GS) the model with grain growth and settling. Note how grain evolution affects the depletion of molecules onto grains near the midplane of cold outer disk (*Vasyunin et al.* (2011)). Middle panel: Gas-phase methanol abundances in a T Tauri disk calculated with a laminar gas-grain chemical model (left) and a 2D turbulent mixing chemical model (right). The transport of methanol ice from dark midplane to upper, more UV-irradiated disk layer enables more methanol ice to be desorbed in the gas phase (*Semenov and Wiebe* (2011)). Bottom panel: Gas-phase methanol abundances in a T Tauri disk calculated with two gas-grain chemical models: (left) no surface chemistry is taken account and (right) with surface chemistry (*Walsh et al.* (2010)). The surface hydrogenation of CO leads to efficient production of methanol ice, which can be partly UV-desorbed in disk layers above midplane.

X-ray luminosity of the T Tauri stars is $\log(L_{\rm X}/L_{\rm bol}) \approx -3.5$ or $L_{\rm X} \approx 3\,10^{29}$ erg s^{-1} (with an uncertainty of an order of magnitude (see e.g. *Preibisch et al.* 2005; *Getman et al.* 2009). This radiation is generated by coronal activity, driven by magnetic fields generated by an $\alpha\omega$ dynamo mechanism in convective stellar interiors. Herbig Ae stars have weak surface magnetic fields due to their non-convective interiors. Their typical X-ray luminosities are $\gtrsim 10$ times lower than those of T Tauri stars (*Güdel and Nazé* 2009). The key role of X-rays in disk chemistry is their ability to penetrate through a high gas columns ($\sim 0.1-1$ g cm^{-2}) and ionize He, which destroys tightly bound molecules like CO, and replenishes gas with elemental carbon and oxygen. The similar effect for disk chemistry is provided by cosmic-ray particules (CRPs), which can penetrate even through very high gas columns, ~ 100 g cm^{-2} (*Umebayashi and Nakano* 1980; *Gammie* 1996; *Cleeves et al.* 2013a).

In the terrestrial planet-forming region, $\sim 1-10$ AU, temperatures are $\gtrsim 100$ K and densities may exceed 10^{12} cm^{-3}. Despite intense gas-grain interactions, surface processes do not play a role and disk chemistry is determined by fast gas-phase reactions, which reaches quickly a steady-state. In the absence of intense sources of ionizing radiation and high temperatures neutral-neutral reactions with barriers become important (*Harada et al.* 2010). At the densities $\gtrsim 10^{12}$ cm^{-3} 3-body reactions also become important (*Aikawa et al.* 1999).

The outer disk regions ($\gtrsim 10$ AU) can be further divided into 3 chemically different regimes (*Aikawa and Herbst* 1999): (1) cold chemistry in the midplane dominated by surface processes, (2) rich gas-grain chemistry in the warm intermediate layer, and (3) restricted PDR-like gas-phase chemistry in the atmosphere.

In the disk atmosphere stellar UV radiation and the interstellar radiation field ionize and dissociate molecules and drive gas-phase PDR-like chemistry. Adjacent to the disk surface a warm, $\approx 30-300$ K, molecular layer is located. This region is partly shielded from stellar and interstellar UV/X-ray radiation, and chemistry is active in the gas and on the dust surfaces. The ionization produces ions, like H_3^+, driving rapid proton transfer and other ion-molecule processes (*Herbst and Klemperer* 1973; *Watson* 1974; *Woodall et al.* 2007; *Wakelam et al.* 2012). If water is frozen onto dust grains, a relatively high C/O ratio close to or even larger than 1 can be reached in the gas phase, leading to a carbon-based chemistry. Ices are released from grains by thermal or photodesorption.

In the outer midplane, the cosmic ray particles and locally produced UV photons are the only ionizing sources. The temperature drops below $\sim 20-50$ K and freeze-out of molecules and hydrogenation reactions on grain surfaces are dominating the chemistry. The most important desorption process for volatiles such as CO, N_2, and CH_4 is thermal desorption. In addition, cosmic ray and X-ray spot heating may release mantle material back to the gas phase (*Leger et al.* 1985; *Hasegawa and Herbst* 1993; *Najita et al.* 2001), as well as reactive desorption (*Garrod et al.* 2007). In the outer, cold disk regions addition of nuclear-spin-dependent chemical reactions involving ortho- and para-states of key species is required.

4.1 Line Emission and Thermo-Chemical Models

Increasing detections of molecular, atomic and ionic emission lines from ground-based infrared and (sub)mm facilities and *Spitzer* and *Herschel* space observatories have led to a recent shift in emphasis on modeling the *gas* structure in disks.

Gas line emission is sensitive to both the abundances of trace emitting species (and hence chemistry) and the excitation conditions (density, temperature, irradiation) at the surface. Meanwhile, the dominant cooling process which controls the gas temperature in the disk surface is radiative cooling by transition lines (e.g. OI, CII, Ly α). Therefore, we need to treat chemistry and thermal processes self-consistently in order to obtain gas temperature structure and predict line fluxes. Thermo-chemical models are important also in order to understand photoevaporation process as a gas dispersal mechanism from disks (*Gorti and Hollenbach* 2009; *Gorti et al.* 2009, see also Chapter by Espaillat et al.).

4.1.1 Thermo-Chemical Models

Early disk models assumed that the gas temperature was equal to that of the dust. In the surface layers, however, low densities and/or heating of gas by stellar X-ray/UV radiation result in weaker thermal coupling of gas to dust and gas and dust temperatures can significantly differ. This is more so in disks where the dust has evolved and the collisional cross-sections are lower (see Sect.4.2.1). Importantly, the vertical density distribution is determined by the gas thermal pressure gradient. These considerations have given rise to the development of thermo-chemical disk models where the gas and dust temperatures are determined separately and self-consistently solved with chemistry to allow more accurate interpretations of observed line emission (see also *Dullemond et al.* 2007).

The first thermo-chemical models consistently solved for the gas temperature structure coupled with chemistry, using a density distribution derived from the dust radiative transfer and temperature solutions. Temperature of gas deviated significantly from dust in optically thin dust-rich disks (*Kamp and van Zadelhoff* 2001). These models were extended to optically thick disks (*Kamp and Dullemond* 2004) and it was determined that gas/dust temperatures were well-coupled in the midplane but not in the higher optically thin dust surface. UV heating was found to be important in the thermally decoupled regions, probed by molecules such as H_2O, CO and OH. *Jonkheid et al.* (2004, 2007) considered the effects of dust evolution to find that dust settling and the resulting increased decoupling allowed gas temperatures to rise; this often increased the intensities of atomic and molecular lines. While these studies focused

on UV heating of gas, Glassgold and collaborators (e.g. *Glassgold et al.* 2004, 2007, 2009, 2012; *Meijerink et al.* 2008; *Najita et al.* 2011) have been examining the effect of X-rays on gas heating and chemistry with increasing levels of detail. X-ray heating dominates surface gas heating in these models and leads to ionization deep in the disk, driving ion-molecule chemistry and the formation of water and other organics. *Glassgold et al.* (2007) predicted an important strongly emitting tracer of ionized gas, the mid-infrared line of [NeII] at 12.8μm. The primary conclusion of these investigations is that disk structure closely resembles photo-dissociation regions (PDRs and XDRs), with a cold, shielded molecular interior and warmer, atomic/ionic surface regions.

A further refinement to thermo-chemical models was to self-consistently solve for vertical hydrostatic equilibrium in the disk as set by the gas temperature structure (*Gorti and Hollenbach* 2004, 2008; *Nomura and Millar* 2005; *Aikawa and Nomura* 2006; *Nomura et al.* 2007) and to consider irradiation of the disk surface by both UV and X-rays (*Gorti and Hollenbach* 2004, 2008; *Nomura et al.* 2007; *Akimkin et al.* 2013). Gas in the surface layer is hotter than the dust grains, which results in a more vertically extended disk atmosphere.

The increased UV/X-ray attenuation in the inner disk lowers the surface gas temperature at intermediate and larger radii compared to the solutions obtained without a gas-determined equilibrium density structure. X-ray heating is found to dominate in the surface layers of disks, often heating gas to $\gtrsim$ 1000-5000K in the inner disk, while FUV heating and both X-ray and UV photodissociation are important in the intermediate ($A_V \sim 0.1 - 1$) regions. Dust thermal balance dominates in the dense, shielded interior layers, although ionization by hard X-ray photons can drive ion-molecule chemistry even in the denser regions of the disk. The change in temperature obtained with a self-consistent density determination is inferred to affect the calculated intensities of molecular and atomic line emission from disks.

More recently *Akimkin et al.* (2013) have introduced a state-of-the-art thermo-chemical ANDES model, which treats time-dependent chemical reactions self-consistently with gas and dust thermal processes and calculations of dust coagulation, fragmentation and settling (see Sect.4.2.1).

4.1.2 Modeling Line Emission

Recent development of thermo-chemical models focused more on modeling observable line emissions from disks. *Gorti and Hollenbach* (2008) found that [NeII] and [ArII] lines are tracers of X-ray ionized regions, and that X-rays and FUV are both significant contributors to gas heating. They concluded that [OI] 63μm line was a strong, luminous coolant in disks. *Nomura et al.* (2007) investigated the strength of various H_2 lines, including dust coagulation calculations, to suggest that infrared line ratios of rovibrational transitions of H_2 are sensitive to gas temperature and FUV radiation field, and could be useful tracer of grain evolution in the surface layers of the inner disks.

In order to statistically model and predict line fluxes from disks for observations by Herschel, ALMA, and forthcoming facilities, a tool, called the DENT grid, was developed to calculate line fluxes with a large number of parameters, such as stellar mass, age, and UV excess, disk masses, scale heights, inner and outer radii, dust properties, and inclination angles, as a part of the Herschel open-time key program of GASPS (*Woitke et al.* 2010; *Kamp et al.* 2011). The DENT grid used the 3D Monte Carlo radiative transfer code, MCFOST (*Pinte et al.* 2006, 2009) for calculating dust temperature and line radiative transfer, and the thermo-chemical model, ProDiMo, for calculating gas temperature and abundances of species. ProDiMo is a sophisticated model which takes into consideration all of the processes mentioned in the previous subsection. *Woitke et al.* (2009b) utilized full 2-D dust continuum transfer, a modest chemical network, and computed the gas temperature and density structure (in 1+1D), but initially only including UV heating and simplified photochemistry. These were updated to improve upon the calculations of the rates of photoprocesses and line radiative transfer (*Kamp et al.* 2010). X-ray irradiation was added in *Aresu et al.* (2011) and *Meijerink et al.* (2012). *Thi et al.* (2011c) studied the effects of the inner rim structure on the disk. These models have been successfully applied to observational data of Herschel GASPS objects of protoplanetary disks and debris disks to infer the important disk properties, such as dust evolution, radial extent, and disk masses (*Meeus et al.* 2010; *Thi et al.* 2011b; *Tilling et al.* 2012; *Podio et al.* 2013).

Bruderer et al. (2009) developed another thermo-chemical disk model. *Bruderer et al.* (2012) adapted it to a disk around a Herbig Be star, HD 100546, and used it to explain the high-J CO lines and the [OI] 63μm line observed by Herschel, together with an upper limit on the [CI] 370 μm line (by APEX). They discussed the variability of the gas/dust ratio and the amount of volatile carbon in the disk atmosphere. *Chapillon et al.* (2008) adopted the Meudon PDR code (*Le Bourlot et al.* 1993; *Le Petit et al.* 2006) with a number of variable parameters such as UV field, grain size, gas-to-dust ratio to explain millimeter CO line observations towards Herbig Ae disks.

While the thermo-chemical models have been developed, the non-LTE line radiative transfer methods for calculating transition lines from disks also have been studied. In *Pavlyuchenkov et al.* (2007) the comparison between various approximate line radiative transfer approaches and a well-tested accelerated Monte Carlo code was performed. Using a T Tauri-like flared disk model and various distributions of molecular abundances (layered and homogeneous), the excitation temperatures, synthetic spectra, and channel maps for a number of rotational lines of CO, $C^{18}O$, HCO^+, DCO^+, HCN, CS, and H_2CO were simulated. It was found that the LTE approach widely assumed by observers is accurate enough for modeling the low molecular rotational lines, whereas it may significantly overestimate the high-J

line intensities in disks. The full escape probability (FEP) approach works better for these high-J rotational lines but fails sometimes for the low-J transitions. *Semenov et al.* (2008) adopted the code to simulate the ALMA observations of maps of molecular line emission from disks, using the resulting molecular abundance profiles of their calculations of chemical reactions.

Brinch and Hogerheijde (2010) developed a line radiative transfer code, LIME, based on the RATRAN code (*Hogerheijde and van der Tak* 2000), in which grids are laid out adaptive to the opacity. Therefore, the code can deal with objects having inhomogeneous 3D structure with large density contrast as well as overlapping lines of multiple species. The code is available on the website: http://www.nbi.dk/∼brinch/lime.php. The LIME code is used in the ARTIST software package designed to model 2D/3D line and continuum radiative transfer and synthesize interferometric images (*Padovani et al.* 2012, http://youngstars.nbi.dk/artist/Welcome.html).

Non-LTE effects are more significant for higher transition lines whose critical densities are high. *Meijerink et al.* (2009) modeled mid-infrared water lines observed by Spitzer (*Rothman et al.* 2005) and showed that the differences in line fluxes obtained by LTE and non-LTE calculations are within an order of magnitude for most of the lines. (*Woitke et al.* 2009a) also studied water line fluxes, including the submillimeter lines and using their full thermochemical model. They showed that the differences are smaller for low excitation water lines.

4.2 Chemistry vs. Physical Processes

Dynamical processes which lead to planet formation, such as grain evolution and gas dispersal, affect chemical structure in protoplanetary disks. Thus, these processes as well as some environmental effects could appear in molecular line emission from the disks.

4.2.1 Effect of Grain Evolution

Grain size distributions in protoplanetary disks are thought to be very different from that of the interstellar grains because of coagulation, settling towards the disk midplane and transport towards the central star under the influence of the gravity of the star (see chapter by Testi et al.).

One of the recent advancement in studies of disk chemistry is the treatment of grain evolution. Grain growth depletes the upper disk layers of small grains and hence reduces the opacity of disk matter, allowing the far-UV radiation to penetrate more efficiently into the disk, and to heat and dissociate molecules deeper in the disk. Also, larger grains populating the disk midplane will delay the depletion of gaseous species because of the reduced total surface area (*Aikawa and Nomura* 2006; *Fogel et al.* 2011; *Vasyunin et al.* 2011). Grain coagulation, fragmentation, sedimentation, turbulent stirring and radial transport are all important processes to control the grain size distribution.

Nomura et al. (2007) investigated the effect of dust evolution only on gas temperature profile and molecular hydrogen excitation by using the result of calculations of coagulation equation with settling of dust particles. *Vasyunin et al.* (2011) studied the effect on chemical reactions, taking into account the fragmentation and cratering of dust particles in addition.

Akimkin et al. (2013) have developed the ANDES model, which is based on combined description of the 1+1D continuum radiative transfer, detailed 2D dust evolution model, and time-dependent laminar chemistry. This model was applied to investigate the impact of grain evolution on disk chemistry. It was found that due to grain growth and dust removal from the disk atmosphere, the molecular layer shifts closer toward the disk midplane that remains shielded by dust from the ionizing radiation. Larger grains settled to the midplane lower the frequency of gas-grain collisions, and thus making depletion of gaseous molecules less severe and hindering the growth of ices on grains.

4.2.2 Chemo-Dynamical Models

Gas in protoplanetary disks is thought to disperse in $1 - 10$ Myr. Magneto-rotational instability driven turbulence will cause angular momentum transfer and the gas accretes towards the central star as a result, while photoevaporation disperses the gas in the region where the thermal energy is high enough for the gas to escape from the gravity of the central star (see chapters by Turner et al., Alexander et al. and Espaillat et al.). The gas motion associated with this gas dispersal process is expected to affect the chemical structure, especially near the boundaries between the three layers: photon-dominated surface layer, warm molecular-rich middle layer, and cold molecule-depleted layer near the midplane. The effect appears significant when the timescale of the gas motion is shorter than the timescales of the dominant chemical reactions. So far, in addition to laminar disk models, a number of chemo-dynamical models of protoplanetary disks have been developed.

On the other hand, chemo-dynamical models have been also developed to treat chemistry in dynamically evolving early phase of star and disk formation where circumstellar disks are still embedded in dense envelope. Some information in this early phase could remain of chemistry in protoplanetary disks after the surrounding envelope clears up, especially of the ice molecules on grains.

In the coming years, we expect that sophisticated multi-dimensional magneto-hydrodynamical models will be coupled with time-dependent chemistry. First steps in this direction have been made (*Turner et al.* 2007), where a simple chemical model has been coupled to a local 3D MHD simulation.

4.2.2.1 Turbulent Mixing and Gas Accretion

Chemical evolution in protoplanetary disks with 1D radial advective mass transport was studied by *Woods and*

Willacy (2007, 2009a); *Willacy and Woods* (2009); *Nomura et al.* (2009). Another class of chemo-dynamical disk models is based on turbulent diffusive mixing, which uniformises chemical gradients, and is modeled in 1D, 2D, or even full 3D (*Ilgner and Nelson* 2006a,b,c, 2008; *Semenov et al.* 2006; *Aikawa* 2007; *Semenov and Wiebe* 2011; *Willacy et al.* 2006; *Hersant et al.* 2009; *Turner et al.* 2006, 2007). In several disk models both advective and turbulent transport was considered (*Heinzeller et al.* 2011), while *Gorti et al.* (2009) studied photoevaporation of disks and loss of the gas due to the stellar far-UV and X-ray radiation.

The turbulence in disks is a 3D-phenomenon driven by a magneto-rotational instability (*Balbus and Hawley* 1991, ,see also Turner et al. chapter in this book). Global MHD simulations show that advection has no specified direction in various disk regions, and in each location goes both inward and outward. The corresponding turbulent velocity of the gas $V_{\rm turb}$ depends on the viscosity parameter α (*Shakura and Sunyaev* 1973) and scales with it somewhere between linear and square-root dependence: $\alpha < V_{\rm turb}/c_{\rm s} < \sqrt{\alpha}$, here $c_{\rm s}$ is the sound speed. The calculated α-viscosity stresses have values in a range of 10^{-4} and 10^{-2} in the midplane and the molecular layer, respectively, and rise steeply to transonic values of ~ 0.5 in the disk atmosphere.

MRI requires a modest gas ionization to be operational. The ionization structure of protoplanetary disks is largely controlled by a variety of chemical processes. Recent studies of the chemistry coupled to the dynamics in protoplanetary disks are briefly summarized below (see also Sect. 5.1). *Ilgner and Nelson* (2006c) have studied the ionization structure of inner disks ($r < 10$ AU), considering vertical mixing and other effects like X-ray flares, various elemental compositions, etc. They found that mixing has no profound effect on electron concentration if metals are absent in the gas since recombination timescales are faster than dynamical timescales. However, when $T \gtrsim 200$ K and alkali atoms are present in the gas, chemistry of ionization becomes sensitive to transport, such that diffusion may reduce the size of the turbulent-inactive disk "dead" zone (see also Sect. 5.2).

Willacy et al. (2006) have attempted to study systematically the impact of disk diffusivity on evolution of various chemical families. They used a steady-state α-disk model similar to that of *Ilgner et al.* (2004) and considered 1D-vertical mixing in the outer disk region with $r > 100$ AU. They found that vertical transport can increase column densities (vertically integrated concentrations) by up to 2 orders of magnitude for some complex species. Still, the layered disk structure was largely preserved even in the presence of vertical mixing. *Semenov et al.* (2006) and *Aikawa* (2007) have found that turbulence allows to transport gaseous CO from the molecular layer down towards the cold midplane where it otherwise remains frozen out, which may explain the large amount of cold ($\lesssim 15$ K) CO gas detected in the disk of DM Tau (*Dartois et al.* 2003). *Hersant et al.* (2009) have studied various mechanisms to retain gas-phase CO in very cold disk regions, including vertical mixing. They found that photodesorption in upper, less obscured molecular layer greatly increases the gas-phase CO concentration, whereas the role of vertical mixing is less important.

Later, in *Woods and Willacy* (2007) the formation and destruction of benzene in turbulent protoplanetary disks at $r \lesssim 35$ AU has been investigated. These authors found that radial transport allows efficient synthesis of benzene at $\lesssim 3$ AU, mostly due to ion-molecule reactions between C_3H_3 and $C_3H_4^+$ followed by grain dissociative recombination. The resulting concentration of C_6H_6 at larger radii of $10 - 30$ AU is increased by turbulent diffusion up to 2 orders of magnitude.

In a similar study, *Nomura et al.* (2009) have considered a inner disk model with radial advection ($\lesssim 12$ AU). They found that the molecular concentrations are sensitive to the transport speed, such that in some cases gaseous molecules are able to reach the outer, cooler disk regions where they should be depleted. This increases the production of many complex or surface-produced species such as methanol, ammonia, hydrogen sulfide, acetylene, etc.

Tscharnuter and Gail (2007) have considered a 2D disk chemo-hydrodynamical model in which global circulation flow patterns exist, transporting disk matter outward in the disk midplane and inward in elevated disk layers. They found that gas-phase species produced by warm neutral-neutral chemistry in the inner region can be transported into the cold outer region and freeze out onto dust grain surfaces. The presence of such large-scale meridional flows in protoplanetary accretion disks was called in question in later MHD studies *Fromang et al.* (2011); *Flock et al.* (2011).

Heinzeller et al. (2011) have studied the chemical evolution of a protoplanetary disk with radial viscous accretion, vertical mixing, and a vertical disk wind (in the atmosphere). They used a steady-state disk model with $\alpha = 0.01$ and $\dot{M} = 10^{-8}\,M_\odot\,{\rm yr}^{-1}$. They found that mixing lowers concentration gradients, enhancing abundances of NH_3, CH_3OH, C_2H_2 and sulfur-containing species. They concluded that such a disk wind has an effect similar to turbulent mixing on chemistry, while the radial accretion changes molecular abundances in the midplane, and the vertical turbulent mixing enhances abundances in the intermediate molecular layer.

A detailed study of the effect of 2D radial-vertical mixing on gas-grain chemistry in a protoplanetary disk has been performed in *Semenov and Wiebe* (2011). These authors used the α-model of a ~ 5 Myr DM Tau-like disk coupled to the large-scale gas-grain chemical code "ALCHEMIC" (*Semenov et al.* 2010). To account for production of complex molecules, an extended set of surface processes was added. A constant value of the viscosity parameter $\alpha = 0.01$ was assumed.

In this study it was shown that turbulent transport changes the abundances of many gas-phase species and particularly ices. Vertical mixing is more important than radial mixing, mainly because radial temperature and density gradients in disks are weaker than vertical ones. The

simple molecules not responding to dynamical transport include C_2H, C^+, CH_4, CN, CO, HCN, HNC, H_2CO, OH, as well as water and ammonia ices. The species sensitive to transport are carbon chains and other heavy species, in particular sulfur-bearing and complex organic molecules (COMs) frozen onto the dust grains. Mixing transports ice-coated grains into warmer disk regions where efficient surface recombination reactions proceed. In warm molecular layer these complex ices evaporate and return to the gas phase.

4.2.2.2 Dynamics in Early Phase

In protostellar phase, materials in envelopes surrounding circumstellar disks dynamically fall onto the disks, and then accrete towards the central star in the disks. Chemical evolution, including gas-grain interaction, along 2D advection flow from envelopes to disks was studied by *Visser et al.* (2009, 2011). Using axisymmetric 2D semi-analytical dynamical models, they discussed the origin of organic molecules and other species in comets in our Solar System.

Assumption of axisymmetry will be adoptable for quiescent disks where mass is transported locally with low accretion rates, but may be inappropriate for disks in the early phase, which are massive enough to trigger gravitational instabilities (*Vorobyov and Basu* 2006). Gravitational instabilities produce transient non-axisymmetric structures in the form of spiral waves, density clumps, etc... (*Boley et al.* 2010; *Vorobyov and Basu* 2010). The results of Vorobyov and collaborators have been confronted by *Zhu et al.* (2010a,b, 2012), who found that ongoing accretion of an envelope surrounding a forming protoplanetary disks can alone drive non-stationary accretion and hence outbursts similar to the FU Ori phenomenon. More importantly, gravitational instabilities lead to efficient mass transport and angular momentum redistribution, which could be characterized by a relatively high viscosity parameter $\alpha \sim 1$. *Ilee et al.* (2011) performed a first study of time-dependent chemistry along paths of fluid elements in 3D radiative hydrodynamical simulations of a gravitationally unstable massive disk ($0.39M_\odot$ within a disk radius of 50 AU) by *Boley et al.* (2007) and showed importance of continuous stirring by rotating spiral density waves with weak shocks on chemical properties in the disk.

4.2.3 Environmental Effects

Since chemical processes are sensitive to local density, temperature, and radiation fields, we expect to see different chemical structure and molecular line emission if a protoplanetary disk is in a specific environment.

Cleeves et al. (2011) investigated the chemical structure of a transition disk with a large central hole (with a radius of 45 AU). Transition disks are interesting objects to study dispersal mechanisms of disks, for example, by giant planets and/or photoevaporation, and so on (see chapters by Espaillat et al. and Alexander et al., and Sect. 5.4). *Cleeves et al.* (2011) showed that the inner edge of the disk is heated by direct irradiation from the central star so that the even molecules with high desorption energies can survive in the gas-phase near the midplane. Line radiative transfer calculations predicted that this actively evolving truncation region in transition disks will be probed by observations of high transition lines of such molecules by ALMA with high spatial resolution.

Walsh et al. (2013b) studied the chemical structure of a protoplanetary disk irradiated externally by a nearby massive star. Although it is observationally suggested that stars are often formed in young star clusters (e.g. *Lada and Lada* 2003), star and planet formation in isolated systems have been mainly studied because detailed observations have been available only isolated star forming regions close to our Sun so far. However, ALMA is expected to provide detailed (sub)millimeter observations of protoplanetary disks in young clusters, such as the Trapezium cluster in the Orion nebula, allowing us to study star and planet formation in varied environments. *Walsh et al.* (2013b) showed that external irradiation from nearby OB stars can heat gas and dust even near the disk midplanes, especially in the outer regions, affecting snowlines of molecules with desorption temperature of $\sim$30K. Also, due to the externally irradiated FUV photons, the ionization degree becomes higher in the disk surface. Predictions of molecular line emission showed observations of line ratios will be useful to probe physical and chemical properties of the disk, such as ionization degree and photoevaporation condition.

Cleeves et al. (2013a) investigated the ionization rate in protoplanetary disks excluded by cosmic rays. It has been suggested that strong winds from the central young star with strong magnetic activity may decrease cosmic-ray flux penetrating into the disks by analogy with the solar wind modulating cosmic-ray photons in our Solar System. *Cleeves et al.* (2013a) showed that the ionization rate by cosmic-ray can be reduced by stellar winds to a value lower than that due to short-lived radionuclides of $\zeta_{\rm RN} \sim 10^{-18}{\rm s}^{-1}$ (*Umebayashi and Nakano* 2009), with which magnetorotational instability will be locally stabilized in the inner disk.

4.3 New advances in treatment of chemical processes

4.3.1 Photochemistry

Under the strong UV and X-ray irradiation from the central star, photochemistry is dominant in the surface layers of protoplanetary disks. A detailed 2D/3D treatment of the X-ray and UV radiation transfer with anisotropic scattering is an essential ingredient for realistic disk chemical models (e.g. *Igea and Glassgold* 1999; *van Zadelhoff et al.* 2003). The photochemistry dominant region expands in the disks with grain evolution as dust opacities become lower at UV wavelengths. In heavily irradiated disk atmospheres many species will exist in excited (ro-)vibrational states, which may then react differently with other species and require addition of state-to-state processes in the models (*Pierce and A'Hearn* 2010).

An accurately calculated UV spectrum including Lyα resonant scattering is required to calculate photodissociation and photoionization rates, and shielding factors for CO, H_2, and H_2O (*Bethell and Bergin* 2009, 2011). *Fogel et al.* (2011) adopt their Ly α and UV continuum radiation field to time-dependent chemistry in disks with grain settling to show that the Ly α radiation impacts the column densities of HCN, NH_3, and CH_4, especially when grain settling is significant.

Walsh et al. (2012) studied the impact of photochemistry and X-ray ionization on the molecular composition in a disk to show that detailed treatment of X-ray ionization mainly affects N_2H^+ distribution, while the shape of the UV spectrum affects distribution of many molecules in the outer disk.

Photodesorption of molecules from icy mantles on grains is also an important mechanism in the surface and middle layer of protoplanetary disks. The photodesorption rates were recently derived experimentally for CO, H_2O, CH_4, and NH_3 (*Öberg et al.* 2007, 2009a,b; *Fayolle et al.* 2011). *Walsh et al.* (2010) showed by a chemical model in a protoplanetary disk that photodesorption significantly affects molecular column densities of HCN, CN, CS, H_2O and CO_2 (see also *Willacy* 2007; *Semenov and Wiebe* 2011).

4.3.2 Chemistry of Organic Molecules

Although various complex organic molecules, such as glycoaldehyde and cyanomethanimine (e.g. *Zaleski et al.* 2013), have been detected towards luminous hot cores and hot corinos, H_2CO, HC_3N (*Chapillon et al.* 2012b), and c-C_3H_2 (*Qi et al.* 2013a) are the largest molecules detected towards less luminous protoplanetary disks so far. On the other hand, more complex organic molecules have been found in our Solar System by infrared and radio observations towards comets (e.g. *Mumma and Charnley* 2011), in a sample return mission from the comet 81P/Wild2 (STARDUST, *Elsila et al.* 2009), and in meteorites. It is an interesting topic to investigate how these complex molecules were formed in the early Solar System.

Since the detection of mid-infrared lines of small organic molecules and water by Spitzer Space Telescope (e.g. *Carr and Najita* 2008), they have been treated in many chemical models of protoplanetary disks (e.g. *Woods and Willacy* 2009b; *Nomura et al.* 2009; *Woitke et al.* 2009a). *Agúndez et al.* (2008) pointed out an importance of gas phase synthesis with molecular hydrogen to form carbon-bearing organic molecules, while *Glassgold et al.* (2009) indicated that water abundance is significantly affected by molecular hydrogen formation rate from which water is mainly formed through gas-phase reaction in warm disk atmosphere. *Heinzeller et al.* (2011) showed that transport of molecular hydrogen from UV-photon-shielded molecular-rich layer to hot disk surface by turbulent mixing enhances abundances of water and small organic molecules.

Meanwhile, more complex organic molecules, which have not been detected towards protoplanetary disks yet, are believed to form on grain surfaces (e.g. *Herbst and van Dishoeck* 2009). *Walsh et al.* (2010) showed that grain surface chemistry together with photodesorption enhances gas-phase complex organic molecules, such as HCOOH, CH_3OH, and $HCOOCH_3$ in the middle layer of the outer disk. Also, *Semenov and Wiebe* (2011) showed that grain surface chemistry and then organic molecule formation are affected by turbulent mixing. *Walsh et al.* (2013a) treated further complex grain surface chemistry (following *Garrod and Herbst* (2006) and *Garrod et al.* (2008)) which includes heavy-radical recombination reactions efficient on warm grains together with photodesorption, reactive desorption, and photodissociation of ice on grains. They showed that complex organic molecules are formed by the surface reactions on warm grains near the midplane at the disk radius of $\geq$20AU. The resulting grain-surface fractional abundances are consistent with those observed towards comets. Also, they predict based on model calculations of transition lines that strong methanol lines will be excellent candidates for ALMA observations towards disks.

4.4 Sensitivity Analysis and intrinsic uncertainties of chemical Models

To improve our knowledge of the physics and chemistry of protoplanetary disks, it is necessary to understand the robustness of the chemical models to the uncertainties in the reaction rate coefficients, which define the individual reaction efficiency. Sensitivity methods have been developed for such purposes and applied to several types of sources (*Vasyunin et al.* 2004; *Wakelam et al.* 2005, 2010). Those methods follow the propagation of the uncertainties during the calculation of the abundance species. Error bars on the computed abundances can be determined and "key" reactions can be identified. *Vasyunin et al.* (2008) applied such methods for protoplanetary disk chemistry, showing that the dispersion in the molecular column densities is within an order of magnitude at 10^6 yrs when chemical reactions are in a quasi-equilibrium state. Abundances of some molecules could be very sensitive to rate uncertainties, especially those of X-ray ionization rates in specific regions.

Results of model calculations of chemical reactions also depend on the applied chemical network in some degree. Chemical networks used for disk chemistry are usually derived from the public networks UMIST (*McElroy et al.* 2013, http://www.udfa.net/)) and OSU (http://www.physics.ohio-state.edu/$\sim$eric/research.html). Those two networks have been developed and updated over the years since the 1990s. The latest version of the OSU network has recently been published under the name of kida.uva.2011 (*Wakelam et al.* 2012), being updated from the online database KIDA (http://kida.obs.u-bordeaux1.fr/). The UMIST network contains a number of chemical reactions with activation barriers, and even 3-body assisted reactions, that can become important in the inner regions of the disks. The OSU/kida.uva network is primarily designed for the outer parts of the disk were the temperatures stay be-

low 300 K. Additions have been done to the OSU network by *Harada et al.* (2010, 2012) to use it up to temperatures of about 800 K. In *Wakelam et al.* (2012), differences in the resulting molecular abundances computed by different chemical networks were studied in a dense cloud model to show that errors are typically within an order of magnitude. It is worth noticing that these networks contain approximate values for the gas-phase molecular photodissociation rates which are valid for the UV interstellar radiation field only. Photorates for different star spectra have been published by *van Dishoeck et al.* (2006) (see also *Visser et al.* 2009).

Contrary to the gas-phase, there is up to now no detailed database of surface reactions for the interstellar medium. Only a few networks have been put online by authors. Some of them can be found on the KIDA website (http://kida.obs.u-bordeaux1.fr/models).

5. TOWARDS THE ALMA ERA

5.1 Measuring the turbulence

Turbulence is a key ingredient for the evolution and composition of disks.

On one hand, the turbulence strength, more precisely the α viscosity parameter, can be derived indirectly through its impact on disk spreading (*Guilloteau et al.* 2011) and dust settling (*Mulders and Dominik* 2012). From the (dust) disk shapes and sizes at mm wavelengths (which sample the disk midplane), *Guilloteau et al.* (2011) found $\alpha \simeq 10^{-3} - 10^{-2}$ at a characteristic radius of 100 AU, possibly decreasing with time. IR SED analyses, which sample the top layers and are more sensitive to 10 AU scales, provided similar values, although the derived α depends on the assumed grain sizes and gas-to-dust ratio (*Mulders and Dominik* 2012).

On another hand, high resolution spectroscopy can directly probe the magnitude of turbulence, by separating the bulk motions (Keplerian rotation) from local broadening and isolating the thermal and turbulent contributions to this broadening. For spatially unresolved spectra, turbulent broadening can smear out the double-peaked profiles expected for Keplerian disk. This property was used by *Carr et al.* (2004), who found supersonic turbulence from CO overtone bands in SVS13, but lower values from H_2O lines, suggesting a highly turbulent disk surface in the inner few AUs.

With spatially resolved spectro-imaging, the Keplerian motions lead to iso-velocity regions which follow an arc shape, given by

$$r(\theta) \quad = \quad (GM_*/V_{\rm obs}^2) \sin^2 i \cos^2 \theta. \qquad (2)$$

The dynamical mass and disk inclination control the curvature, while local broadening controls the width of the emission across the arc. Thus, local broadening is easily separated from the Keplerian shear, and can be recovered usually through a global fit of a (semi-)parametric disk model. Using the PdBI, local line widths of order $0.05 - 0.15$ km/s were found in the early work of *Guilloteau and Dutrey* (1998) using CO observations of DM Tau, and subsequently for LkCa15 and MWC 480 by *Piétu et al.* (2007). Work by *Qi et al.* (2004) found that a smaller linewidth in the range 0.05-0.1 km/s was required to reproduce CO J=3-2 observations of the TW Hya disk. Using CO isotopologues, *Dartois et al.* (2003) suggested the turbulence could be smaller in the upper layers of the disk, a result not confirmed by *Piétu et al.* (2007) for LkCa15 and MWC 480 (see also *Dutrey et al.* 2008, for GM Aur). Similar values were reported from other molecular tracers such as CN, HCN (*Chapillon et al.* 2012a), or HCO^+ (*Piétu et al.* 2007). The inferred turbulent velocities are subsonic, Mach $\simeq 0.1 - 0.5$, which corresponds to viscosity α values of $\simeq 0.01 - 0.1$ (*Cuzzi et al.* 2001).

These initial measurements suffered from several limitations: one is sensitivity, resulting in only CO being observed at high S/N, another is the spectral resolution, and the third is the limited knowledge of the thermal line width. Several authors, including *Piétu et al.* (2007), *Isella et al.* (2007), and *Qi et al.* (2008) have particularly noted the difficulty of meaningfully constraining turbulent linewidths whose magnitudes are comparable to the spectral resolution of the data. *Hughes et al.* (2011) utilized the higher spectral resolution provided by the SMA correlator to measure the non-thermal broadening of the CO lines in TW Hya and HD 163296. They used a two independent thermal structures to derive consistent estimates of turbulent broadening that achieve consistent results: one derived from modeling the SED of the stars to estimate the temperature in the CO emitting layer, and one freely variable parametric model. Their results indicate a very small level of turbulence in TW Hya, $< 0.04\,{\rm km.s^{-1}}$, but a substantially higher value in HD 163296 ($0.3\,{\rm km.s^{-1}}$).

Because of its high optical depth, CO unfortunately only samples a very thin layer high up in the disk atmosphere. Measurements with other, optically thinner, tracers are essential to probe the turbulence across the disk. However, the distribution of molecules like CN is insufficiently well understood to remove the thermal component. For CN (and also C_2H), the apparent excitation temperatures are found to be low, 10 – 15 K (*Henning et al.* 2010; *Chapillon et al.* 2012a), while the temperature in the molecular rich layer is expected to be around 20-30 K, high enough to contribute significantly to the local line width. To minimize the contribution of thermal motions to the local line width such that the turbulence component can be measured, *Guilloteau et al.* (2012) used CS, a relatively "heavy" molecule ($\mu = 44$, compared to $25 - 28$ for CN, CCH or CO). Observing the J=3-2 transition with the IRAM PdBI, and with accurate modeling of the correlator response, they derive a turbulent width of $0.12{\rm km.s^{-1}}$, and show this value to be robust against the unknowns related to the CS spatial distribution (kinetic temperature, location above disk plane). It corresponds to a Mach number of order 0.5, a value which is only reached at several scale heights above the disk plane

in MHD simulations (e.g. *Fromang and Nelson* 2006; *Flock et al.* 2011), while chemical models predict CS to be around 1-2 scale heights.

All measurements so far provide disk-averaged values. The radial variations are as yet too poorly constrained: assuming a power law radial distribution for the turbulent width, *Guilloteau et al.* (2012) inferred an exponent 0.38 ± 0.45, which can equally accommodate a constant turbulent velocity, or a constant Mach number. It is also worth emphasizing that the "turbulent" width is an adjustable parameter to catch (to first order) all deviations around the mean Keplerian motion, as could occur in case of e.g. spiral waves or disk warps (see for example the complex case of AB Aur in the papers by *Piétu et al.* (2005) and *Tang et al.* (2012)).

The extremely limited number of sources studied so far precludes any general conclusion to be drawn from the relation between non-thermal linewidth and, e.g. disk size (which would be expected due to viscous evolution), stellar mass (which determines the spectrum of ionizing radiation), or evolutionary state (transitional or non-transitional). Substantial progress is expected with ALMA, which will provide much higher sensitivity, higher spectral resolution, and higher angular resolution, but also the possibility to use transitions with different optical depths to probe different altitudes above the disk plane. The CS molecule is well suited for this, along with a number of other rotational lines falling in the ALMA bands.

5.2 Estimating the Ionization and Dead Zone

One of the most important properties of protoplanetary disks is their ionization structure which is until now poorly constrained by the observations. Weakly ionized plasma in rotating configuration is subject to the magnetorotational instability (MRI) (e.g. *Balbus and Hawley* 1991), which is thought to drive turbulence in disks. Turbulence causes anomalous viscosity of the gas and thus enables angular momentum transport and regulates the global disk evolution. It is operational even at very low ionization degree values of $\lesssim 10^{-10}$ in the inner disk midplane regions completely shielded from the external UV/X-ray radiation (but rarely from the cosmic ray particles), see also *Cleeves et al.* (2013b). In massive enough disks the inner region can be shielded even from the CRPs, either due to magnetospherical activity of the central star or by a high obscuring gas column of $\gtrsim 100$ g cm^{-3} (*Umebayashi and Nakano* 1980; *Gammie* 1996; *Cleeves et al.* 2013a). This leads to the formation of a "dead zone" with damped turbulence, through which transport of matter is severely reduced (see, e.g. *Sano et al.* 2000; *Semenov et al.* 2004; *Flock et al.* 2012b; *Martin et al.* 2012; *Mohanty et al.* 2013; *Dzyurkevich et al.* 2013). This has implications on the efficiency of grain growth and their radial migration (*Hasegawa and Pudritz* 2010a; *Meheut et al.* 2012a), planet formation (*Oishi et al.* 2007), disk chemistry and physics (*Suzuki et al.* 2010; *Lesniak and Desch* 2011; *Flock et al.* 2012a), development of spiral waves, gaps, and other asymmetric structures (*Meheut et al.* 2010; *Morishima* 2012; *Meheut et al.* 2012b; *Gressel et al.* 2012).

Even with modern computational facilities, the complex interplay between weakly charged plasma and magnetic fields in disks is very difficult to simulate in full glory of detail. *Ilgner and Nelson* (2006b,c) investigated in detail ionization chemistry in disks and its sensitivity to various physical and chemical effects at $r < 10$ AU: (1) the X-ray flares from the young T Tauri star (*Ilgner and Nelson* 2006c), and (2) the vertical turbulent mixing transport and the amount of gas-phase metals (*Ilgner and Nelson* 2006b). Using an α-disk model with stellar X-ray-irradiation, they demonstrated that the simple network from *Oppenheimer and Dalgarno* (1974), using 5 species only, tends to overestimate the ionization degree since metals exchange charges with polyatomic species, and that magnetically decoupled "dead" region may exist in disks as long as small grains and metals are removed from gas. The vertical diffusion has no effect on the electron abundances when the metals are absent in the gas because recombination timescales for polyatomic ions are rapid. When the dominant ions are metals, the characteristic ionization timescale becomes so long that the ionization chemistry becomes sensitive to transport, which drastically reduces the size of the "dead" zone. In the disk model with sporadic X-ray flares (by up to a factor of 100 in the luminosity) the outer part of the "dead" zone disappears, whereas the inner part of the "dead" zone evolves along with variations of the X-ray flux.

The first attempts to model self-consistently disk chemical, physical, and turbulent structures in full 3D have been performed by *Turner et al.* (2006) and *Ilgner and Nelson* (2008). Both studies have employed a shearing-box approximation to calculate a patch of a 3D MHD disk at radii of $\sim 1 - 5$ AU, treated the development of the MRI-driven turbulence, and focused on the multi-fluid evolution of the disk ionization state.

Ilgner and Nelson (2008) have confirmed their earlier findings (*Ilgner and Nelson* 2006a,b) that turbulent mixing has no effect on the disk ionization structure in the absence of the gas-phase metals. The presence of metals, however, prolongs the recombination timescale, and the mixing is thus able to enliven the "dead" zone at $r \geq 5$ AU (with the resulting $\alpha = 1 - 5 \times 10^{-3}$).

The first 3D-MHD disk model coupled with a limited time-dependent ionization chemistry was made by *Turner et al.* (2007). They have again confirmed that large-scale turbulent transport brings charged particles and radial magnetic fields toward the midplane, resulting in accretion stresses there that are only a few times lower than in the active surface layers. Later, *Flaig et al.* (2012) have performed local 3D radiative MHD simulations of different radii of a protosolar-like disk, including a simplified chemical network with recombination of charged particles on dust grains in the presence of the stellar X-rays, cosmic rays and the decay of radionuclides. They have found that at the distance between 2 to 4 AU a "dead zone" appears.

A detailed study of the global gas-grain ionization chemistry in the presence of turbulent mixing for a DM Tau-like disk model has been performed by *Semenov and Wiebe* (2011). It was found that the turbulent diffusion does not affect abundances of simple metal ions and a molecular ions such as C^+, Mg^+, Fe^+, He^+, H_3^+, CH_3^+, NH_4^+. On the other hand, charged species sensitive to the mixing include hydrocarbon ions, electrons, H^+, N_2H^+, HCO^+, N^+, OH^+, H_2O^+, etc. They have re-confirmed that the global ionization structure has a layered structure even in the presence of transport processes: (1) heavily irradiated and ionized, hot atmosphere, where the dominant ions are C^+ and H^+, (2) partly UV-shielded, warm molecular layer where carbon is locked in CO and major ions are H^+, HCO^+ and H_3^+, and (3) dark, dense and cold midplane, where most of molecules are frozen out onto dust grains, and the most abundant charged particles are dust grains and H_3^+.

Walsh et al. (2012) have investigated the impact of photochemistry and X-ray ionization on the molecular composition and ionization fraction in a T Tauri disk. The photoreaction rates were calculated using the local UV wavelength spectrum and, the wavelength-dependent photo cross sections. The same approach was utilized to model the transport of the stellar X-ray radiation. They have found that photochemistry is more important for global disk chemistry than the X-ray radiation. More accurate photochemistry affects the location of the H/H_2 and C^+/C dissociation fronts in upper disk layer and increases abundances of neutral molecules in the outer disk region. *Walsh et al.* (2012) concluded that there is a potential "dead zone" with suppressed accretion located within the inner ~ 200 AU midplane region.

Several observational campaigns have begun to test some of these theoretical predictions. *Dutrey et al.* (2007a) have performed high-sensitivity interferometric observations with the IRAM PdBI array of N_2H^+ 1–0 in the disks around DM Tau, LkCa 15, and MWC 480. These data were used to derive the N_2H^+ column densities and, together with the HCO^+ measurements, were compared with a steady-state disk model with a vertical temperature gradient coupled to a gas-grain chemistry network. The derived N_2H^+/HCO^+ ratio is on the order of $0.02 - 0.03$, similar to the value observed in colder and darker prestellar cores. The observed values qualitatively agree with the modeled column densities at a disk age of a few million years, but the radial distribution of the molecules were not reproduced. The estimated ionization degree values from the HCO^+ and N_2H^+ data are $\sim 2 - 7 \times 10^{-9}$ (wrt the total hydrogen density), which are typical for the warm molecular layers in the outer disk regions.

Öberg et al. (2011b) have presented interferometric observations with SMA of CO 3–2 in the DM Tau disk, and upper limits on H_2D^+ $1_{1,0} - 0_{1,1}$ and N_2H^+ 4–3. With these data, IRAM 30-m observations of $H^{13}CO^+$ 3–2, and previous SMA observations of N_2H^+ 3–2, HCO^+ 3–2, and DCO^+ 3–2 (see *Öberg et al.* 2010), they constrained ionization fraction using a parametric physical disk model. They have found that: (1) in a warm molecular layer ($T > 20$ K) HCO^+ is the dominant ion and the ionization degree is $\sim 4 \times 10^{-10}$, (2) in a cooler layer around midplane where CO is depleted ($\lesssim 15 - 20$ K) N_2H^+ and DCO^+ are the dominant ions, and the fractional ionization is $\sim 3 \times 10^{-11}$, and (3) in the cold, dense midplane ($T < 15$ K) the isotopologues of H_3^+ are the main charge carriers, and the fractional ionization drops below $\sim 3 \times 10^{-10}$. These observations confirm that the disk ionization degree decreases towards deeper, denser and better shielded disk regions. Unfortunately, the best tracer of the ionization in the disk midplane, ortho-H_2D^+, still remains to be firmly detected in protoplanetary disks (see Sect.5.3 and Chapter of Ceccarelli et al.).

5.3 Deuteration

Deuterated molecules are important tracers of the thermal and chemical history in protoplanetary disks and the ISM (see also the chapter by Ceccarelli et al. in this book). The cosmic D/H ratio in the local ISM is D/H$\approx 1.5\,10^{-5}$ (*Linsky et al.* 2006), with a major reservoir of D locked in HD in dense regions. The deuterium fractionation processes redistribute the elemental deuterium from HD to other species at low temperatures, enhancing abundances and D/H ratios of many polyatomic species by orders of magnitude, as observed in the cold ISM (e.g. *Bacmann et al.* 2003; *Bergin and Tafalla* 2007; *Henning and Semenov* 2013).

This is due to the difference in zero point vibrational energy between the H-bearing and D-bearing species, which implies barriers for backward reactions and thus favors production of deuterated species. The key process for gas-phase fractionation at $T \lesssim 10 - 30$ K is deuterium enrichment of H_3^+: $H_3^+ + HD \leftrightarrows H_2D^+ + H_2 + 232$ K (*Millar et al.* 1989; *Gerlich et al.* 2002). Upon fractionation of H_3^+, proton exchange reactions transfer the D enhancement to more complex gaseous species. One of the key reactions of this kind in protoplanetary disks is the formation of DCO^+: $H_2D^+ + CO \leftrightarrows DCO^+ + H_2$, which produces an enhanced DCO^+/HCO^+ ratios at in outer cold disk midplanes (at $\sim 10 - 30$ K). A similar reaction produces N_2D^+ in the coldest regions where gaseous CO is frozen-out: $H_2D^+ + N_2 \leftrightarrows N_2D^+ + H_2$.

In the outer midplane regions where CO and other molecules are severely depleted, multiply-deuterated H_3^+ isotopologues attain large abundances (*Albertsson et al.* 2013). Upon dissociative recombination large amounts of atomic H and D are produced. Atomic hydrogen and deuterium can then stick to grain surfaces and hydrogenate or deuterate the first generation of relatively simple ices. After that, CRP-driven/UV-driven photo- and thermal processing of ice mantles allow more complex (organic) deuterated ices to be synthesized (e.g. multiply-deuterated H_2O, H_2CO, CH_3OH, HCOOH, etc.).

Another pathway to redistribute the elemental D from HD via gas-phase fractionation is effective at higher tem-

peratures, $\lesssim 70-80$ K: CH_3^+ + HD $\leftrightarrows$ CH_2D^+ + H_2 + 390 K (*Asvany et al.* 2004) and $C_2H_2^+$ + HD $\leftrightarrows$ C_2HD^+ + H_2 + 550 K (*Herbst et al.* 1987). After that, DCN molecules can be produced : N + $CH_2D^+ \rightarrow DCN^+ + H_2$, followed by protonation of DCN^+ by H_2 or HD and dissociative recombination of $DCNH^+$ (*Roueff et al.* 2007).

Only three deuterated species have been detected in disks: DCO^+, DCN, and HD. The detection of the ground transition $1_{0,1} - 0_{0,0}$ of HDO in absorption in the disk of DM Tau by *Ceccarelli et al.* (2005) was later refuted by *Guilloteau et al.* (2006), and remains unproven. DCO^+ was first detected in the TW Hya disk (*van Dishoeck et al.* 2003; *Qi et al.* 2008), then in DM Tau by *Guilloteau et al.* (2006), and LkCa15 by *Öberg et al.* (2010). The interpretation of the apparent $[DCO^+]/[HCO^+]$ ratio, ~ 0.02, is not simple, as HCO^+ is in general optically thick (e.g. *Öberg et al.* 2011a), and both molecules have different spatial distributions (*Öberg et al.* 2012).

DCN has been detected so far in two disks: in TW Hya by *Qi et al.* (2008) and in LkCa 15 by *Öberg et al.* (2010). The SMA and ALMA Science Verification observations show different spatial distributions of DCN and DCO^+, which imply different formation pathways (see *Qi et al.* 2008; *Öberg et al.* 2012). Deuteration for DCN proceeds more efficiently through proton exchange with deuterated light hydrocarbons like CH_3^+, whereas for DCO^+ low-temperature fractionation via H_3^+ isotopologues is important (see above).

Recently, the far-infrared fundamental rotational line of HD has been detected in the TW Hya disk with *Herschel* (*Bergin et al.* 2013). The abundance distribution of HD closely follows that of H_2. Therefore, HD, which has a weak permanent dipole moment, can be used for probing disk gas mass. The inferred mass of the TW Hya disk is $\gtrsim 0.05 M_\odot$, which is surprising for a $\sim 3-10$Myr-old system.

Among deuterated molecular species, H_2D^+ is potentially a critical probe of diskc midplanes, where it can be a dominant charged species (*Ceccarelli and Dominik* 2005). It is rapidly destroyed by the ion-molecule reactions with CO and other molecules, and abundant enough only in the high density cold midplane regions, where most of the molecules are frozen onto grains. Its lowest transition is unfortunately at 372 GHz, where the atmospheric transparency is limited. Current searches failed to detect it, the initial tentative reports of *Ceccarelli et al.* (2004) being superseded by 3 times more sensitive upper limits of *Chapillon et al.* (2011) using the JCMT and APEX in DM Tau and TW Hya. *Chapillon et al.* (2011) compared the upper limit with the prediction from several disk models, varying the density, temperature and outer radius), grain sizes (0.1, 1 and 10 μm), CO abundances (10^{-4},10^{-5} and 10^{-6}) and rate of cosmic rays ionization (10^{-17}, 3.10^{-17} and 10^{-16} s^{-1}). The data only firmly exclude cases with both a low CO abundance and small grains. This study also indicates that H_2D^+ is more difficult to detect than expected, and that even with the full ALMA, significant integration times will be needed to probe the physics and chemistry of the cold depleted midplane of T Tauri disks through H_2D^+ imaging.

5.4 Gas in Inner Cavities

It is worth mentioning that (sub)mm observations are in some cases sensitive to the gaseous content of the inner disks. The simple way that comes to mind is the use of observations spatially resolving the inner disk (whatever arbitrary size an "inner disk" refers to). Unless the inner region under consideration is large, this requires a very fine angular resolution, which limits its applicability to the bright disks (and bright lines) and large holes. However, it is not necessary to spatially resolve the inner parts of the disk to have access to its content. Since disks are geometrically thin with a well ordered velocity field, there is a mapping between velocity axis and position within the disks. Specifically, in a Keplerian disk, the line wings originate from the inner parts, so e.g. the absence of high-velocity wings indicates an inner truncation. However the line wings are also fainter than the core which makes such analysis challenging from a sensitivity point of view. Another complication arises from the fact this flux density from this wings is comparable if not weaker to the continuum flux density, calling for both a very good bandpass calibration and continuum handling.

The archetype of a large inner hole lies at the center of GG Tau, the famous multiple system, with a circumbinary ring surrounding GG Tau A. *Dutrey et al.* (1994); *Guilloteau et al.* (1999) found that the dust and the gas circumbinary ring plus disk had the same inner radius. *Guilloteau and Dutrey* (2001) later found ^{12}CO 2–1 emission within the ring that possibly traces streaming material from the circumbinary ring feeding the circumprimary disks that would otherwise disappear through accretion of their material onto the host stars.

A handful of other systems have been imaged at high angular resolution in molecular lines, providing interesting complementary information to that of the continuum (see Chapter by Espaillat et al.). For example, *Piétu et al.* (2007) found from CO 2–1 observations that CO is present in the inner part of LkCa 15 disk where dust emission present a drop in emissivity a situation similar to the AB Aur system (*Piétu et al.* 2006; *Tang et al.* 2012).

Using a spectroscopic approach, *Dutrey et al.* (2008) analyzed the J=2-1 line emission of CO isotopologues in the GM Aur disk (PdBI data), and used a global fit to the data to overcome the sensitivity issue. They could show that the inner radius in CO was comparable to that of the dust (*Hughes et al.* 2009). A similar method was used to infer the presence of an inner gas cavity in the 40 Myr-old 49 Ceti system (*Hughes et al.* 2008). More recently, *Rosenfeld et al.* (2012) performed a similar analysis on TW Hya taking advantage of the brightness of the relatively close system and enhanced sensitivity of the ALMA array. This allowed them to not only trace CO down to about 2 AU from the central star, but also to point out that simple model fails to repro-

duce the observed line wings calling for alternative models such as, e.g. a warped inner disk.

ALMA is already providing examples of the kind of structures that may be present in the inner disk, by the analogous examples at larger radii. Using ALMA, *Casassus et al.* (2013) were able to image multiple molecular gas species within the dust inner hole of HD 142527 and utilize the varying optical depths of the different species to detect a flow of gas crossing the gap opened by a planet while *van der Marel et al.* (2013) recently imaged a dust trap in the disk surrounding Oph IRS 48. Over the next several years, ALMA will likely uncover similar structures, and many more unexpected ones, at radii between a few and 30 AU.

5. SUMMARY AND OUTLOOK

Since PPV, thermo-chemical models of disks, as chemical models, have been significantly improved but the detection rate of new molecules in disks has not significantly increased. However, there are some trends which appear from the recent observational results. Among them, it is important to mention:

- So far, only simple molecules have been detected, the most complex being HC_3N and c-C_3H_2, showing that progress in understanding the molecular complexity in disks will require substantial observational efforts, even with ALMA. Similarly, the upper limits obtained on H_2D^+ indicate that probing the disk midplane will be difficult.

- Multi-line, multi-isotopologue CO interferometric studies allow observers and modelers to retrieve the basic density and temperature structures of disks. This method will become more and more accurate with ALMA.

- The CO, CN, HCN, CS and CCH molecular studies apparently reveal low temperatures in the gas phase in several T Tauri disks. These observations suggest that the molecular layer is at least partly colder than predicted and that there are some ingredients still missing in our understanding of the disk physics and/or chemistry. More accurate ALMA data will refine these studies.

- Dust is one of the major agent shaping the disk physics and chemistry. In particular, it plays a fundamental role to control the UV disk illumination and hence the temperature. It also strongly influences the chemistry since a significant part of the disk is at a temperature which is below the freeze out temperature of most molecules. Although substantial progress has been made in the chemical modeling, a more comprehensive treatment of chemical reactions on grain surface remains to be incorporated.

- Deriving the total amount of gas mass is the most difficult task because the bulk of the gas, H_2, cannot be directly traced. The recent detection of HD with Herschel is therefore very promising. In the near future, GREAT on SOFIA may allow detection of HD lines in other disks. Probing the gas-to-dust ratio will be then an even more complex step, as recent dust observations reveal that the dust properties also changes radially. ALMA will fortunately provide a better accuracy on the observable aspect of dust properties, the emissivity index.

- With an adequate angular resolution and sensitivity, ALMA will provide the first images of inner dust and gas disks ($R \leq 30$ AU), revealing the physics and chemistry of the inner part. In particular, these new observations will provide the first quantitative constrain on the ionization status, the turbulence and the kinematics in the planet forming area, as any departure to 2D-symetry.

Acknowledgments. Anne Dutrey would like to acknowledge all CID members for a very fruitful collaboration, in particular Th.Henning, R.Launhardt, F.Gueth and K.Schreyer. We also thank all the KIDA team (http://kida.obs.u-bordeaux1.fr) for providing chemical reaction rates for astrophysics. Anne Dutrey and Stéphane Guilloteau thank the French Program PCMI for providing financial support. Dmitry Semenov acknowledges support by the Deutsche Forschungsgemeinschaft through SPP 1385: The first ten million years of the solar system - a planetary materials approach (SE 1962/1-2 and 1962/1-3).

REFERENCES

Agúndez M. et al. (2008) *Astron. Astrophys*, *483*, 831.
Aikawa Y. (2007) *Astrophys. J*, *656*, L93.
Aikawa Y. and Herbst E. (1999) *Astron. Astrophys*, *351*, 233.
Aikawa Y. and Nomura H. (2006) *Astrophys. J*, *642*, 1152.
Aikawa Y. et al. (1999) *Astrophys. J*, *519*, 705.
Aikawa Y. et al. (2002) *Astron. Astrophys*, *386*, 622.
Akimkin V. et al. (2013) *Astrophys. J*, *766*, 8.
Albertsson T. et al. (2013) *Astrophys. J. Suppl.*, *207*, 27.
Aresu G. et al. (2011) *Astron. Astrophys*, *526*, 163.
Aresu G. et al. (2012) *Astron. Astrophys.*, *547*, A69.
Asvany O. et al. (2004) *Astrophys. J*, *617*, 685.
Bacmann A. et al. (2003) *Astrophys. J*, *585*, L55.
Balbus S. A. and Hawley J. F. (1991) *Astrophys. J*, *376*, 214.
Bergin E. et al. (2003) *Astrophys. J*, *591*, L159.
Bergin E. A. (2011) *The Chemical Evolution of Protoplanetary Disks*, pp. 55–113.
Bergin E. A. and Tafalla M. (2007) *Annu. Rev. Astron. Astrophys.*, *45*, 339.
Bergin E. A. et al. (2010) *Astron. Astrophys*, *521*, L33.
Bergin E. A. et al. (2013) *Nature*, *493*, 644.
Bethell T. and Bergin E. (2009) *Science*, *326*, 1675.
Bethell T. J. and Bergin E. A. (2011) *Astrophys. J*, *739*, 78.

Boley A. C. et al. (2007) *Astrophys. J.*, *665*, 1254.
Boley A. C. et al. (2010) *Icarus*, *207*, 509.
Brinch C. and Hogerheijde M. R. (2010) *Astron. Astrophys.*, *523*, A25.
Bruderer S. et al. (2009) *Astrophys. J*, *700*, 872.
Bruderer S. et al. (2012) *Astron. Astrophys*, *541*, A91.
Carr J. S. and Najita J. R. (2008) *Science*, *319*, 1504.
Carr J. S. et al. (2004) *Astrophys. J.*, *603*, 213.
Casassus S. et al. (2013) *Nature*, *493*, 191.
Ceccarelli C. and Dominik C. (2005) *Astron. Astrophys*, *440*, 583.
Ceccarelli C. et al. (2004) *Astrophys. J. Lett.*, *607*, L51.
Ceccarelli C. et al. (2005) *Astrophys. J. Lett.*, *631*, L81.
Chapillon E. et al. (2008) *Astron. Astrophys*, *488*, 565.
Chapillon E. et al. (2011) *Astron. Astrophys*, *533*, A143.
Chapillon E. et al. (2012a) *Astron. Astrophys*, *537*, A60.
Chapillon E. et al. (2012b) *Astrophys. J*, *756*, 58.
Chiang E. I. and Goldreich P. (1997) *Astrophys. J*, *490*, 368.
Cleeves L. I. et al. (2011) *Astrophys. J., Lett*, *743*, L2.
Cleeves L. I. et al. (2013a) *Astrophys. J.*, *772*, 5.
Cleeves L. I. et al. (2013b) *Astrophys. J.*, *777*, 28.
Cuzzi J. N. et al. (2001) *Astrophys. J.*, *546*, 496.
D'Alessio P. et al. (1998) *Astrophys. J*, *500*, 411.
Dartois E. et al. (2003) *Astron. Astrophys*, *399*, 773.
de Gregorio-Monsalvo I. et al. (2013) *Astron. Astrophys.*, *557*, A133.
Draine B. T. (1978) *Astrophys. J*, *36*, 595.
Dullemond C. P. and Monnier J. D. (2010) *Annu. Rev. Astron. Astrophys.*, *48*, 205.
Dullemond C. P. et al. (2007) *Models of the Structure and Evolution of Protoplanetary Disks*, p. 555, University of Arizona Press, Tucson.
Dutrey A. et al. (1994) *Astron. Astrophys.*, *286*, 149.
Dutrey A. et al. (1997) *Astron. Astrophys*, *317*, L55.
Dutrey A. et al. (2003) *Astron. Astrophys.*, *402*, 1003.
Dutrey A. et al. (2007a) *Astron. Astrophys*, *464*, 615.
Dutrey A. et al. (2007b) *Protostars and Planets V*, pp. 495–506.
Dutrey A. et al. (2008) *Astron. Astrophys.*, *490*, L15.
Dutrey A. et al. (2011) *Astron. Astrophys*, *535*, A104.
Dzyurkevich N. et al. (2013) *arXiv:astro-ph/1301.1487*.
Elsila J. E. et al. (2009) *Meteoritics and Planetary Science*, *44*, 1323.
Favre C. et al. (2013) *Astrophys. J. Lett.*, *776*, L38.
Fayolle E. C. et al. (2011) *Astrophys. J*, *739*, L36.
Fedele D. et al. (2012) *Astron. Astrophys.*, *544*, L9.
Fedele D. et al. (2013) *ArXiv:astro-ph/1308.1578*,.
Flaig M. et al. (2012) *Mon. Not. R. Astron. Soc.*, *420*, 2419.
Flock M. et al. (2011) *Astrophys. J*, *735*, 122.
Flock M. et al. (2012a) *Astrophys. J*, *744*, 144.
Flock M. et al. (2012b) *Astrophys. J.*, *761*, 95.
Fogel J. K. J. et al. (2011) *Astrophys. J*, *726*, 29.
Fromang S. and Nelson R. P. (2006) *Astron. Astrophys.*, *457*, 343.
Fromang S. et al. (2011) *Astron. Astrophys.*, *534*, A107.
Gammie C. F. (1996) *Astrophys. J*, *457*, 355.
Garozzo M. et al. (2010) *Astron. Astrophys.*, *509*, A67.
Garrod R. T. and Herbst E. (2006) *Astron. Astrophys*, *457*, 927.
Garrod R. T. et al. (2007) *Astron. Astrophys*, *467*, 1103.
Garrod R. T. et al. (2008) *Astrophys. J.*, *682*, 283.
Gerlich D. et al. (2002) *Planet. Space Sci.*, *50*, 1275.
Getman K. V. et al. (2009) *Astrophys. J*, *699*, 1454.
Glassgold A. E. et al. (2004) *Astrophys. J*, *615*, 972.
Glassgold A. E. et al. (2007) *Astrophys. J*, *656*, 515.
Glassgold A. E. et al. (2009) *Astrophys. J*, *701*, 142x.
Glassgold A. E. et al. (2012) *Astrophys. J*, *756*, 157.
Gorti U. and Hollenbach D. (2004) *Astrophys. J*, *613*, 424.
Gorti U. and Hollenbach D. (2008) *Astrophys. J*, *683*, 287.
Gorti U. and Hollenbach D. (2009) *Astrophys. J.*, *690*, 1539.
Gorti U. et al. (2009) *Astrophys. J*, *705*, 1237.
Gräfe C. et al. (2013) *Astron. Astrophys.*, *553*, A69.
Gressel O. et al. (2012) *Mon. Not. R. Astron. Soc.*, *422*, 1140.
Güdel M. and Nazé Y. (2009) *Astron. Astrophys.*, *17*, 309.
Guilloteau S. and Dutrey A. (1998) *Astron. Astrophys*, *339*, 467.
Guilloteau S. and Dutrey A. (2001) in: *The Formation of Binary Stars*, vol. 200 of *IAU Symposium*, (edited by H. Zinnecker and R. Mathieu), p. 229.
Guilloteau S. et al. (1999) *Astron. Astrophys.*, *348*, 570.
Guilloteau S. et al. (2006) *Astron. Astrophys*, *448*, L5.
Guilloteau S. et al. (2011) *Astron. Astrophys*, *529*, A105.
Guilloteau S. et al. (2012) *Astron. Astrophys*, *548*, A70.
Guilloteau S. et al. (2013) *Astron. Astrophys.*, *549*, A92.
Harada N. et al. (2010) *Astrophys. J*, *721*, 1570.
Harada N. et al. (2012) *Astrophys. J.*, *756*, 104.
Hasegawa T. I. and Herbst E. (1993) *Mon. Not. R. Astron. Soc*, *263*, 589.
Hasegawa Y. and Pudritz R. E. (2010a) *Astrophys. J. Lett.*, *710*, L167.
Hasegawa Y. and Pudritz R. E. (2010b) *Mon. Not. R. Astron. Soc.*, *401*, 143.
Heinzeller D. et al. (2011) *Astrophys. J*, *731*, 115.
Henning T. and Semenov D. (2013) *ArXiv e-prints*.
Henning T. et al. (2010) *Astrophys. J*, *714*, 1511.
Herbst E. and Klemperer W. (1973) *Astrophys. J*, *185*, 505.
Herbst E. and van Dishoeck E. F. (2009) *Ann. Rev. Astron. Astrophys*, *47*, 427.
Herbst E. et al. (1987) *Astrophys. J*, *312*, 351.
Hersant F. et al. (2009) *Astron. Astrophys*, *493*, L49.
Hogerheijde M. R. and van der Tak F. F. S. (2000) *Astron. Astrophys.*, *362*, 697.
Hogerheijde M. R. et al. (2011) *Science*, *334*, 338.
Hughes A. M. et al. (2008) *Astrophys. J.*, *681*, 626.
Hughes A. M. et al. (2009) *Astrophys. J.*, *698*, 131.
Hughes A. M. et al. (2011) *Astrophys. J*, *727*, 85.
Igea J. and Glassgold A. E. (1999) *Astrophys. J*, *518*, 848.
Ilee J. D. et al. (2011) *Mon. Not. R. Astron. Soc*, *417*, 2950.
Ilgner M. and Nelson R. P. (2006a) *Astron. Astrophys*, *445*, 205.
Ilgner M. and Nelson R. P. (2006b) *Astron. Astrophys*, *445*, 223.
Ilgner M. and Nelson R. P. (2006c) *Astron. Astrophys*, *455*, 731.
Ilgner M. and Nelson R. P. (2008) *Astron. Astrophys*, *483*, 815.
Ilgner M. et al. (2004) *Astron. Astrophys*, *415*, 643.
Isella A. et al. (2007) *Astron. Astrophys.*, *469*, 213.
Isella A. et al. (2009) *Astrophys. J.*, *701*, 260.
Jonkheid B. et al. (2004) *Astron. Astrophys*, *428*, 511.
Jonkheid B. et al. (2006) *Astron. Astrophys*, *453*, 163.
Jonkheid B. et al. (2007) *Astron. Astrophys*, *463*, 203.
Kamp I. and Dullemond C. P. (2004) *Astrophys. J.*, *615*, 991.
Kamp I. and van Zadelhoff G.-J. (2001) *Astron. Astrophys*, *373*, 641.
Kamp I. et al. (2010) *Astron. Astrophys.*, *510*, A18.
Kamp I. et al. (2011) *Astron. Astrophys*, *532*, A85.
Kastner J. H. et al. (1997) *Science*, *277*, 67.
Koerner D. W. et al. (1993) *Icarus*, *106*, 2.
Kraus S. et al. (2009) *Astron. Astrophys.*, *508*, 787.
Lada C. J. and Lada E. A. (2003) *Annu. Rev. Astron. Astrophys.*, *41*, 57.
Le Bourlot J. et al. (1993) *Astron. Astrophys.*, *267*, 233.

Le Petit F. et al. (2006) *Astrophys. J. Suppl., 164*, 506.
Leger A. et al. (1985) *Astron. Astrophys, 144*, 147.
Lesniak M. V. and Desch S. J. (2011) *Astrophys. J., 740*, 118.
Linsky J. L. et al. (2006) *Astrophys. J, 647*, 1106.
Maaskant K. M. et al. (2013) *Astron. Astrophys., 555*, A64.
Martin R. G. et al. (2012) *Mon. Not. R. Astron. Soc., 420*, 3139.
Mathews G. S. et al. (2013) *Astron. Astrophys., 557*, A132.
McClure M. K. et al. (2012) *Astrophys. J. Lett., 759*, L10.
McClure M. K. et al. (2013) *Astrophys. J., 775*, 114.
McElroy D. et al. (2013) *Astron. Astrophys., 550*, A36.
Meeus G. et al. (2010) *Astron. Astrophys., 518*, L124.
Meeus G. et al. (2012) *Astron. Astrophys., 544*, A78.
Meheut H. et al. (2010) *Astron. Astrophys., 516*, A31.
Meheut H. et al. (2012a) *Astron. Astrophys, 545*, A134.
Meheut H. et al. (2012b) *Mon. Not. R. Astron. Soc., 422*, 2399.
Meijerink R. et al. (2008) *Astrophys. J, 676*, 518.
Meijerink R. et al. (2009) *Astrophys. J., 704*, 1471.
Meijerink R. et al. (2012) *Astron. Astrophys, 547*, A68.
Millar T.-J. et al. (1989) *Astrophys. J, 340*, 906.
Mohanty S. et al. (2013) *Astrophys. J, 764*, 65.
Morishima R. (2012) *Mon. Not. R. Astron. Soc., 420*, 2851.
Mulders G. D. and Dominik C. (2012) *Astron. Astrophys., 539*, A9.
Mulders G. D. et al. (2011) *Astron. Astrophys., 531*, A93.
Mulders G. D. et al. (2013) *ArXiv e-prints*.
Mumma M. J. and Charnley S. B. (2011) *Annu. Rev. Astron. Astrophys., 49*, 471.
Najita J. et al. (2001) *Astrophys. J, 561*, 880.
Najita J. R. et al. (2011) *Astrophys. J, 743*, 147.
Najita J. R. et al. (2013) *Astrophys. J., 766*, 134.
Nomura H. and Millar T. J. (2005) *Astron. Astrophys, 438*, 923.
Nomura H. et al. (2007) *Astrophys. J, 661*, 334.
Nomura H. et al. (2009) *Astron. Astrophys, 495*, 183.
Öberg K. I. et al. (2007) *Astrophys. J, 662*, L23.
Öberg K. I. et al. (2009a) *Astron. Astrophys, 496*, 281.
Öberg K. I. et al. (2009b) *Astrophys. J, 693*, 1209.
Öberg K. I. et al. (2010) *Astrophys. J, 720*, 480.
Öberg K. I. et al. (2011a) *Astrophys. J, 734*, 98.
Öberg K. I. et al. (2011b) *Astrophys. J, 743*, 152.
Öberg K. I. et al. (2012) *Astrophys. J, 749*, 162.
Oishi J. S. et al. (2007) *Astrophys. J., 670*, 805.
Oppenheimer M. and Dalgarno A. (1974) *Astrophys. J, 192*, 29.
Padovani M. et al. (2012) *Astron. Astrophys., 543*, A16.
Pavlyuchenkov Y. et al. (2007) *Astrophys. J, 669*, 1262.
Pierce D. M. and A'Hearn M. F. (2010) *Astrophys. J, 718*, 340.
Piétu V. et al. (2005) *Astron. Astrophys., 443*, 945.
Piétu V. et al. (2006) *Astron. Astrophys., 460*, L43.
Piétu V. et al. (2007) *Astron. Astrophys, 467*, 163.
Pinte C. et al. (2006) *Astron. Astrophys, 459*, 797.
Pinte C. et al. (2008) *Astron. Astrophys., 489*, 633.
Pinte C. et al. (2009) *Astron. Astrophys., 498*, 967.
Podio L. et al. (2012) *Astron. Astrophys., 545*, A44.
Podio L. et al. (2013) *Astrophys. J. Lett., 766*, L5.
Preibisch T. et al. (2005) *Astrophys. J, 160*, 401.
Qi C. et al. (2004) *Astrophys. J. Lett., 616*, L11.
Qi C. et al. (2006) *Astrophys. J, 636*, L157.
Qi C. et al. (2008) *Astrophys. J, 681*, 1396.
Qi C. et al. (2011) *Astrophys. J., 740*, 84.
Qi C. et al. (2013a) *Astrophys. J. Lett., 765*, L14.
Qi C. et al. (2013b) *Astrophys. J., 765*, 34.
Qi C. et al. (2013c) *Science, 341*, 630.
Riviere-Marichalar P. et al. (2012) *Astron. Astrophys., 538*, L3.
Riviere-Marichalar P. et al. (2013) *Astron. Astrophys., 555*, A67.
Roberge A. et al. (2005) *Astrophys. J., 622*, 1171.
Rosenfeld K. A. et al. (2012) *Astrophys. J., 757*, 129.
Rosenfeld K. A. et al. (2013) *Astrophys. J., 774*, 16.
Rothman L. S. et al. (2005) *J. Quant. Spec. Radiat. Transf., 96*, 139.
Roueff E. et al. (2007) *Astron. Astrophys, 464*, 245.
Sano T. et al. (2000) *Astrophys. J, 543*, 486.
Semenov D. (2010) *ArXiv e-prints*.
Semenov D. and Wiebe D. (2011) *Astrophys. J, 196*, 25.
Semenov D. et al. (2004) *Astron. Astrophys, 417*, 93.
Semenov D. et al. (2005) *Astrophys. J, 621*, 853.
Semenov D. et al. (2006) *Astrophys. J, 647*, L57.
Semenov D. et al. (2008) *Astrophys. J., Lett, 673*, L195.
Semenov D. et al. (2010) *Astron. Astrophys, 522*, A42.
Shakura N. I. and Sunyaev R. A. (1973) *Astron. Astrophys., 24*, 337.
Sturm B. et al. (2010) *Astron. Astrophys., 518*, L129.
Sturm B. et al. (2013) *Astron. Astrophys., 553*, A5.
Suzuki T. K. et al. (2010) *Astrophys. J., 718*, 1289.
Tang Y.-W. et al. (2012) *Astron. Astrophys., 547*, A84.
Thi W.-F. et al. (2004) *Astron. Astrophys, 425*, 955.
Thi W.-F. et al. (2011a) *Astron. Astrophys., 530*, L2.
Thi W.-F. et al. (2011b) *Astron. Astrophys, 530*, L2.
Thi W.-F. et al. (2011c) *Mon. Not. R. Astron. Soc., 412*, 711.
Thi W. F. et al. (2013) *ArXiv e-prints*.
Tilling I. et al. (2012) *Astron. Astrophys., 538*, A20.
Tscharnuter W. M. and Gail H.-P. (2007) *Astron. Astrophys, 463*, 369.
Turner N. J. et al. (2006) *Astrophys. J, 639*, 1218.
Turner N. J. et al. (2007) *Astrophys. J, 659*, 729.
Umebayashi T. and Nakano T. (1980) *PASJ, 32*, 405.
Umebayashi T. and Nakano T. (2009) *Astrophys. J., 690*, 69.
van Boekel R. et al. (2004) *Nature, 432*, 479.
van der Marel N. et al. (2013) *Science, 340*, 1199.
van Dishoeck E. F. (2006) *Proceedings of the National Academy of Science, 103*, 12249.
van Dishoeck E. F. and Black J. H. (1988) *Astrophys. J, 334*, 771.
van Dishoeck E. F. et al. (2003) *Astron. Astrophys., 400*, L1.
van Dishoeck E. F. et al. (2006) *Photoprocesses in protoplanetary disks*, vol. 133 of *Faraday discussion*, p. 231, Royal Society of Chemistry, Cambridge.
van Zadelhoff G.-J. et al. (2003) *Astron. Astrophys, 397*, 789.
Vasyunin A. I. et al. (2004) *Astronomy Letters, 30*, 566.
Vasyunin A. I. et al. (2008) *Astrophys. J, 672*, 629.
Vasyunin A. I. et al. (2011) *Astrophys. J, 727*, 76.
Visser R. et al. (2009) *Astron. Astrophys, 503*, 323.
Visser R. et al. (2011) *Astron. Astrophys, 534*, A132.
Vorobyov E. I. and Basu S. (2006) *Astrophys. J, 650*, 956.
Vorobyov E. I. and Basu S. (2010) *Astrophys. J, 719*, 1896.
Wakelam V. et al. (2004) *Astron. Astrophys., 422*, 159.
Wakelam V. et al. (2005) *Astron. Astrophys., 444*, 883.
Wakelam V. et al. (2010) *Astron. Astrophys., 517*, A21.
Wakelam V. et al. (2012) *Astrophys. J., Suppl. Ser, 199*, 21.
Walsh C. et al. (2010) *Astrophys. J, 722*, 1607.
Walsh C. et al. (2012) *Astrophys. J, 747*, 114.
Walsh C. et al. (2013a) *Astrophys. J.*
Walsh C. et al. (2013b) *Astrophys. J. Lett., 766*, L23.
Watson W. D. (1974) *Astrophys. J, 188*, 35.
Willacy K. (2007) *Astrophys. J, 660*, 441.
Willacy K. and Woods P. M. (2009) *Astrophys. J, 703*, 479.
Willacy K. et al. (2006) *Astrophys. J, 644*, 1202.

Williams J. P. and Cieza L. A. (2011) *Annu. Rev. Astron. Astrophys.*, *49*, 67.
Woitke P. et al. (2009a) *Astron. Astrophys.*, *501*, L5.
Woitke P. et al. (2009b) *Astron. Astrophys*, *501*, 383.
Woitke P. et al. (2010) *Mon. Not. R. Astron. Soc.*, *405*, L26.
Woodall J. et al. (2007) *Astron. Astrophys*, *466*, 1197.
Woods P. M. and Willacy K. (2007) *Astrophys. J*, *655*, L49.
Woods P. M. and Willacy K. (2009a) *Astrophys. J*, *693*, 1360.
Woods P. M. and Willacy K. (2009b) *Astrophys. J.*, *693*, 1360.
Zaleski D. P. et al. (2013) *Astrophys. J. Lett.*, *765*, L10.
Zhang K. et al. (2013) *Astrophys. J.*, *766*, 82.
Zhu Z. et al. (2010a) *Astrophys. J.*, *713*, 1134.
Zhu Z. et al. (2010b) *Astrophys. J.*, *713*, 1143.
Zhu Z. et al. (2012) *Astrophys. J.*, *746*, 110.

This 2-column preprint was prepared with the AAS LaTeX macros v5.2.